Methodological studies for isoseismal analysis

AUTHORS			REVIEW			APPROVAL		
NOM	DATE	VISA	NOM	DATE	VISA	NOM	DATE	VISA
A. Schlupp,	July 12, 2012		T. Camelbeeck (Royal Obs of Belgium) Scientific Committee		In written review	K. Manchuel WP Leader		
Ch. Sira,	July 12, 2012		M. Mucciarelli (Basilicata University) Scientific Committee		In written review	G. Senfaute SIGMA Project Leader		
M. Durrenberger	July 12, 2012							

DISSEMINATION: *Authors; Steering Committee; Work Package leaders, Scientific Committee, Archiving.*

Summary

The final aim of this study, which started in January 2012, is to build a relation between the magnitude-depth parameters and the isoseismals areas based on well-constrained events of the last century in France (metropolitan). This relation will allow estimating the magnitude and depth of event of the 20th century for their use in seismic hazard assessment.

The advantages of this method, which was chosen by BCSF in agreement with EDF, are that it is independent of the epicentre location, epicentre intensity and it is not sensitive to the geometry (elongation, etc.) of the isoseismals. Nevertheless, we want to trace objectively the isoseismals in the way to reduce the uncertainties related to an expert draw or expert interpretation. Therefore, we will use numerical approaches for the isoseismal draw that can be reproducible.

The first step of the study, which is presented in this report, is to generate automatically isoseismals based on observed intensities (IDP). The procedure should work for recent and well-documented earthquakes but also for older events where the number and density of data are lower. The limit of the method will be evaluated in regards to the IDP number and density. This report presents the methodological approach and the first results for isoseismal automatic draw.

We applied several methods on the Rambervillers (22 February 2003, ML=5,4, Mw=4,8) and the Roulans (23 February 2004, ML=5,1) earthquakes. These events are well known (source parameters) and the BCSF have collected numerous macroseismic data and have estimated the related intensities (EMS98). To simulate characteristic datasets of older events with lower dataset, we reduced the number of data for testing the robustness of the approach.

Two main methods have been selected and tested: the IDW (Inverse Distance Weighted) previously used by BCSF in association with expert isoseismal interpretation, and Kriging method, which is nowadays used by INGV team for their mapping.

The preliminary results show that the best results are obtained by the adjusted Kriging approach. Nevertheless, we have still to improve the results induced by the discontinuous isoseismals (incomplete isoseismal cut by a country border of by shore line).
Preliminary results shows promising outcomes for the isoseismals areas converted in “radius of circle of equivalent area”.

1. Introduction:

One of the tasks of the Bureau central sismologique français (BCSF), since 1921, is to estimates the macroseismic intensities on French territory.

After any earthquake of magnitude superior to 3,7 (ML LDG) affecting the French territory, the BCSF collects macroseismic information by individual and collective forms completed by a field survey if damages are observed on constructions. These data are the basis of the BCSF intensity (EMS98 scale since 2000) assessment.
The commune or city is the minimal spatial unit used at this time for the EMS98 intensity, including when data comes from citizen. Therefore the intensity value is geographically referenced at a specific geographical point for each commune, which is the "official" or "administrative" geographical position of the city.

The intensity values are stored in a database, associated with metadata.

The actual isoseismal generation process at BCSF is the following. For that, we use a mapping of the estimated EMS98 value at each city with, in background, an inverse distance interpolation (IDW) between them represented by a colour grid. From that map, an expert draws the isoseismal lines. See figure-Intro below. The result of the isoseismal is then subject to different parameter and expert interpretation. The IDW method will be described in the next chapters.

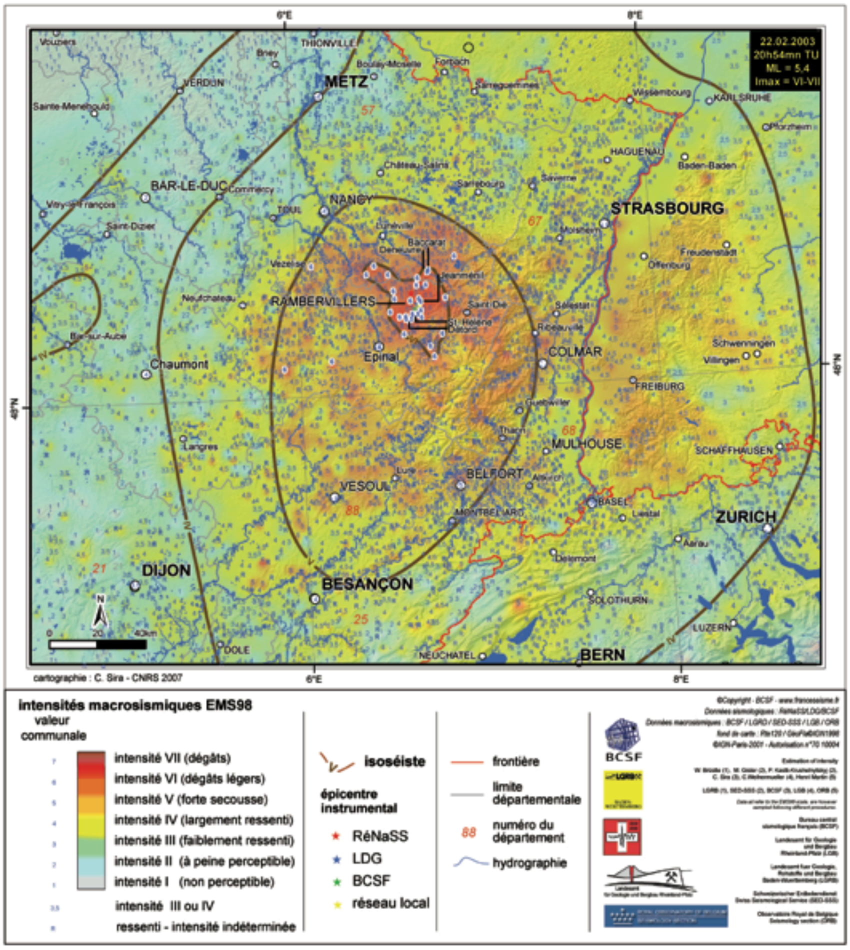

Figure-Intro: Semi-automatic isoseismal mapping (Cara et al. 2005, Cara et al. 2007).

2. Aim of the study.

The final aim of our study in the SIGMA research program is to determine a relation between isoseismal surfaces and magnitude/depth parameters in France based on recent data that are well constrained (revised magnitude Mw, depth constrained and numerous intensities available).

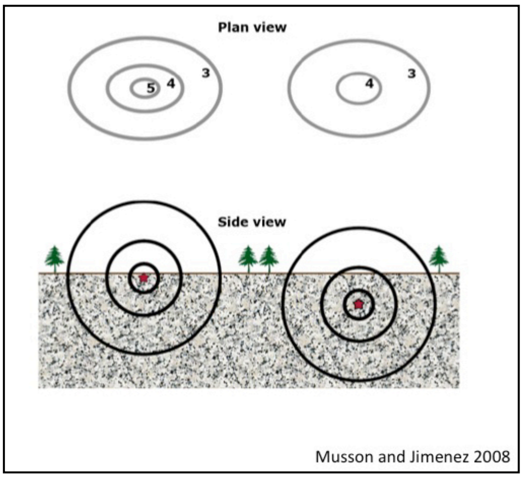

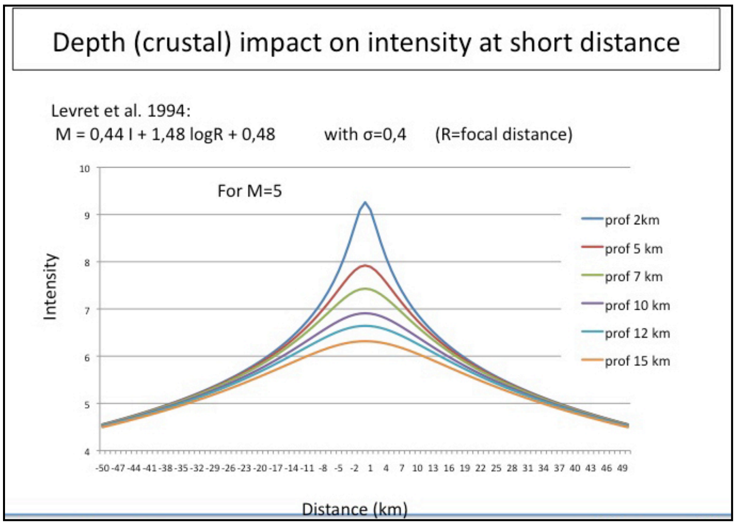

Impact of the depth to the isoseismal area

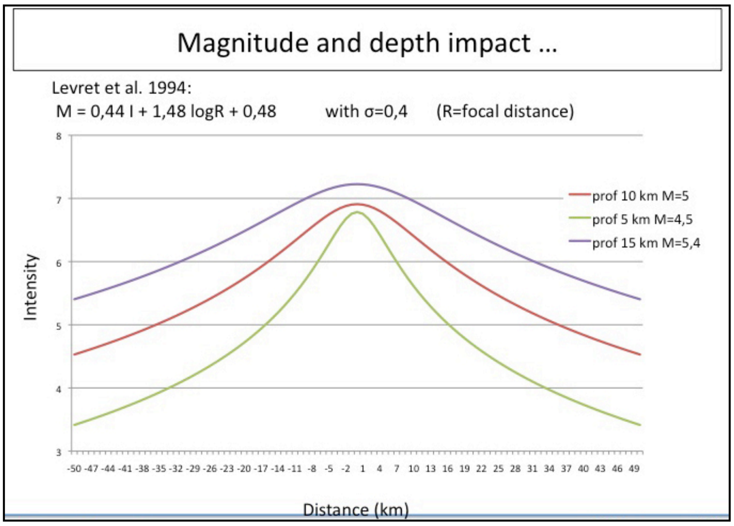

Impact of the magnitude and depth to the isoseismal area

For that, we need first a method to trace the isoseismal that is automatic in the way to avoid the impact on the results of the “expert approach”. The method must be robust and applicable in most real cases, including for event with a smaller number of intensities. This report presents the current progress of our work on the isoseismal automatic draw method, first step of the study.

Our approach is first to determine a method for “automatic” interpolation, which may keep the result as close as possible from the real observed values. Nevertheless, the observed data show clearly local variation of intensity. This variation seems to be mainly due to local effects (site effect) or complex propagation due to heterogeneity in the crust. One other effect could be the low quality of available data that can induce uncertainty on the estimated intensity (over or under estimated). With our experience, this estimation uncertainty seems not to be the main origin of this variation. Nevertheless, in such case, the intensity is associated with a "low quality" code. As we are looking for a relation between source parameters (magnitude-depth) and isoseismal area, we need to smooth these variations, usually the work done by the "expert draw", but without affecting the main trend of the observations.

The first part of the work is then to set up a standard data processing method. It should be customizable, stable, adaptable and valid for a large kind of seismic event. It should be applicable on most events included in the BCSF database.

3. Interpolation methods

Surface interpolation is any formal technique that uses values at sampled locations to predict values at unsampled locations. The values may describe any quantitative geographic phenomenon. Common examples include elevation, rainfall, ozone concentration, temperature, and soil chemistry. In our case, it concern scatter data of intensity located at cities, therefore the region is sampled on a non-regular grid.

The Interpolation operation covers a broad range of interpolation techniques. Several methods of interpolation are available like “Natural Neighborhood”, “Interpolation”, “Bspline” and “kriging”.

We can divide the interpolation methods into two broad groups.

One is a group of deterministic interpolators. This group makes predictions from mathematical formulas that form weighted averages of nearby known values. The methods use different ways to form the weighted averages. This group includes Inverse Distance Weighted (IDW), Global and Local polynomials, and Radial Basis Functions.

The interpolation tool IDW and Spline are directly based on neighbouring observed values or specific mathematical formulae which determine the “smoothed” of the resultant surface. There are several spline types: cubic, bi cubic and thin plate for example. The spline bicubique adjusts the interior of each triangles of Delaunay, a surface the equation of which is a polynomial of rank 3. The method of the thin plate tends to minimize the effort of the surface to pass by the points of the sample.

The other group uses weighted averages as well, but also probability models to calculate predictions. This group includes “Kriging” and all of its different submethods, including “Universal and Indicator Kriging”. Because these methods use probability calculations they are called “stochastic interpolators”.

All methods use the idea of a prediction search neighborhood, where you look at the dozen or so known values that are nearest to the prediction location and discard the rest of the data. This is done for each prediction location, so all the data are used when making an interpolated surface. Here under we present a global overview on interpolation methods that was done at the UCLA resource center (see: http://www.sppsr.ucla.edu/up206b/Interpolation_methods.htm). The various methods are well described in GIS tools. Here under we remind the main idea associated to each. We can find a good overview in the dedicated ArcGis Resource Center. For this chapter 3, we took from it the main part of this interpolation method explanations.
For more details see:
http://help.arcgis.com/en/arcgisdesktop/10.0/help/index.html#/Understanding_interpolation_analysis/009z0000006w000000

3.1. Deterministic interpolators

3.1.1. Inverse Distance Weighted (IDW)

Inverse Distance Weighted (IDW) interpolation implements a basic law of geography, things that are close to one another are more alike than things that are far apart.

To predict a value for any unmeasured location, IDW uses the measured values surrounding the prediction location. Those measured values closest to the prediction location have more influence on the predicted value than those that are farther away (hence the name “inverse distance weighted”). We can determined which values are included in the calculation by specifying and customizing the search neighbourhood, which is the region of the map around a selected point, in which data points are considered for the extrapolation.

IDW assumes that each measured point has some local influence that diminishes with distance. In the figure 1 you can see three different curves that show how fast the influence of a point decays with distance from the prediction location. For the blue curve, all locations (observed data) get the same weight, regardless of how far they are from the prediction location. In the green curve, there is a mild decrease in a point's influence as it gets farther from the prediction location. In the red curve, there is the most dramatic decrease in a point's influence as it gets farther from the prediction location.

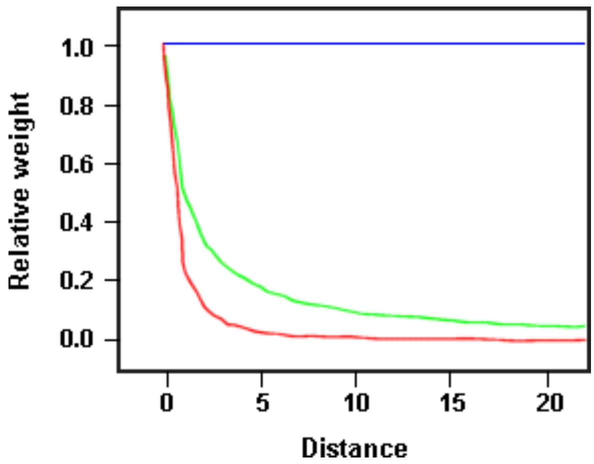

Figure 1 In IDW, the predictive influence (weight) of a measured value depends on its distance from the prediction location. The strength of the dependency can be adjusted.

Notice that as the distance approaches zero, the relative weight approaches one. This means that if one measured point is very close to the prediction location, it will receive almost all of the weight. Thus, IDW is an "exact" interpolator, meaning that the predictions will be exactly equal to the data value when predictions occur at locations where data have already been collected.

3.1.2. Global polynomial

Global polynomial interpolation fits a smooth surface to the sampled data points. In contrast to IDW, it does not use local information. Global polynomial interpolation fits a polynomial regression to the x- and y-coordinates.

Suppose that the elevation data have been collected as in the figure 2. The black points are measured elevation values.

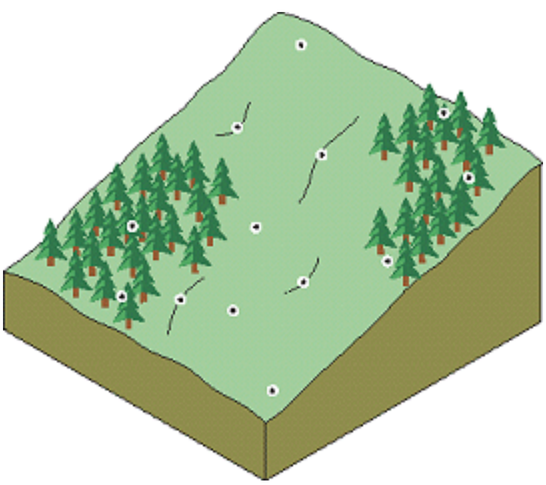

Figure 2: Measured altitude points on the field, black dots, to produce a DEM.

- A *first-order polynomial* fits a rigid plane to the data. Visualize fitting a flat sheet of paper to the elevation points (figure 3). Of course, the elevation values will include lots of little dips and bumps besides the general trend seen in the figure above. The flat surface of a global polynomial will smooth out all of the little bumps. Because the surface is rigid, it will not pass exactly through the sampled data points. This means that the global polynomial is not an exact interpolator; rather, it smoothes over fine-scale details.

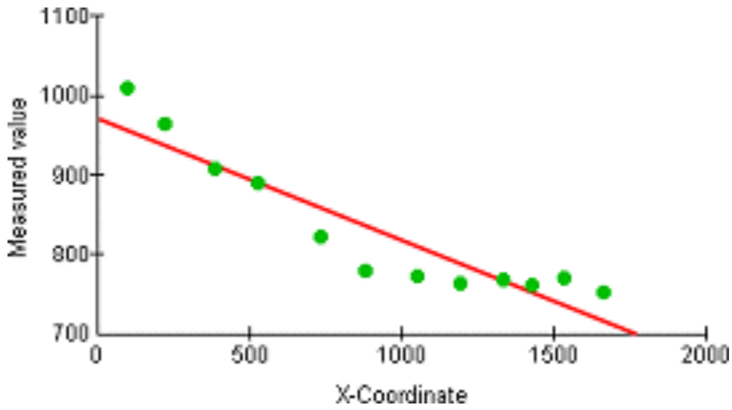

Figure 3: A first order global polynomial surface in cross-section. The surface (red line) captures coarse-scale pattern in the data. It does not pass through the sampled data (green points).

- A flat piece of paper will not represent a landscape with a valley. In that case, you can choose a *second-order polynomial* that lets you "bend" the piece of paper once in one direction (figure 4).

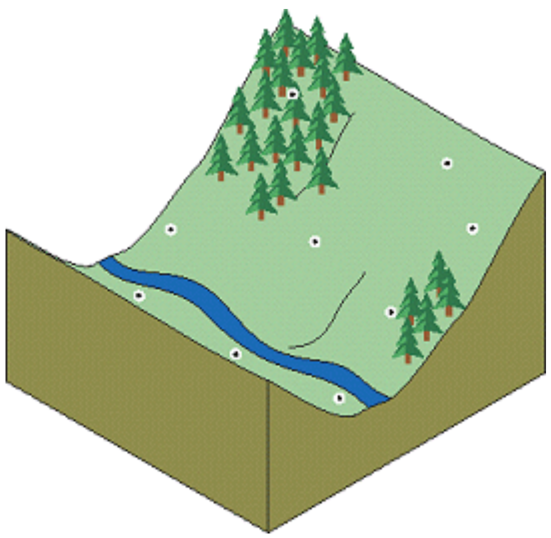

Figure 4: A second-order polynomial allows a single bend in the surface.

Likewise, a third-order polynomial allows two bends and so forth. You can choose up to a tenth-order polynomial in the Geostatistical Analyst. Global Polynomial interpolation is the only method in Geostatistical Analyst that does not use a search neighborhood. If you add the idea of a search neighbourhood to Global Polynomial interpolation, you get Local Polynomial interpolation.

3.1.3. Local polynomial

As described before, global polynomial interpolation creates a surface from a single polynomial formula. Local polynomial interpolation creates a surface from many different formulas; each of them is optimized for a neighborhood.

The neighbourhood shape, maximum and minimum number of points, and sector configuration can be specified. In addition, as with IDW, the sample points in a neighbourhood can be weighted by their distance from the prediction location. Thus, local polynomial interpolation produces surfaces that better account for local variation.

A first-order local polynomial fits a single plane through the data points in the search neighborhood, but keeps only the fitted value at the prediction location. The neighbourhood then slides over to the next prediction location (each neighbourhood thus largely overlaps the ones around it) and the process is repeated. In each case, only the value at the prediction location is kept.

A second-order local polynomial fits a surface with a bend in it to each search neighborhood, a third-order local polynomial fits a surface with two bends to each neighborhood, and so on. Local polynomials are more flexible than global ones. For example, consider the case of a landscape that slopes, levels out, and then slopes again.

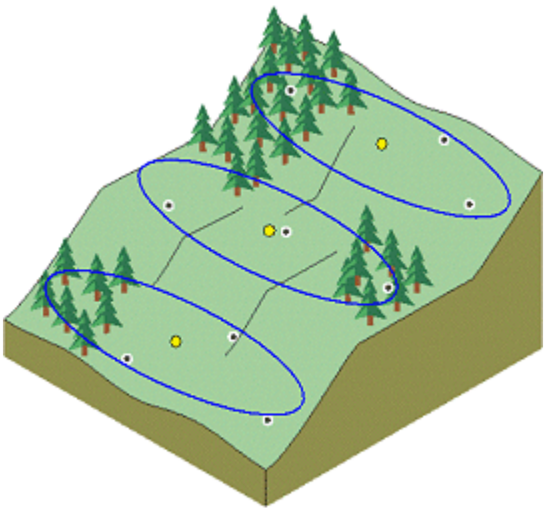

Figure 5: A different plane is fitted to each of the neighbourhoods (blue outlines) that are centred on the prediction locations (yellow points).

A single global polynomial will not fit this landscape very well. Local polynomial interpolation, however, can fit a different plane to each neighbourhood centred on a prediction location. As the interpolator considers each location in turn, the neighbourhoods overlap. The value used for each prediction is that of the fitted polynomial at the centre of the search neighbourhood.

Although it is more flexible than global polynomial interpolation, local polynomial interpolation is not an exact interpolator like IDW.

3.1.4. Radial basis functions

You can think of the surface created by radial basis functions as a rubber membrane that is fitted to each of the measured data points while minimizing the total curvature of the surface. Because the surface must pass through each sampled point, radial basis functions are exact interpolators. Geostatistical Analyst uses five radial basis functions. They are similar, but create slightly different surfaces because they use different math to fit the surface to the sample points.

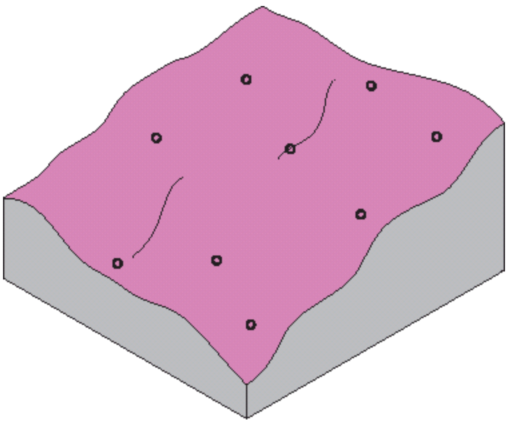

Figure 6: Interpolation using radial basis functions is shown by the purple surface; think of it as a fairly stiff rubber sheet that bends and folds to fit exactly to the sample data points.

3.2. Interpolators based on probability models

The second family of methods of interpolation includes geostatistics techniques (such as the method of kriging), which are based on statistical models including the autocorrelation, that is the statistical relations between the measured points. Consequently, geostatistics techniques have not only the capacity to produce a surface of prediction, but they can also supply measures as for the certainty or the accuracy of these predictions.

3.2.1. Kriging

Kriging wears the name of his precursor, the South African mining engineer D.G. Krige (1951). In the 50s, Krige developed a series of empirical statistical methods to determine the spatial distribution of ores from a set of drillings. It is however French Matheron (1963 and 1972), which formalized the approach by using the correlations between the drillings to consider its spatial distribution. He baptized the method " Kriging ". He was also the first one has to use the term "geostatistics" to indicate the statistical modelling of spatial data. The same ideas were developed, at the same time, in the USSR by L.S. Dandy. Dandy baptized his method "optimal interpolation". He introduced the notion of "objective analysis" to describe this approach based on the correlations. It is the name under which the method is known in meteorology.
In oceanology, Bretherton and al (1976) introduced the method. It is known under the name of "method of interpolation of Gauss-Markov", according to the name that we give him formally in the books of statistics (see Liebelt 1967, for example).

Kriging presents a different way to think about prediction than do the deterministic interpolators. In Kriging, a predicted value depends on two factors: a trend and an additional element of variability. This is an intuitive idea with plenty of analogies in the real world. For instance, if you go from the ocean to the top of a mountain, you have an upward trend in elevation. However, there is likely to be variation on the way—you will go both up and down when crossing valleys, streams, knobs and other features.

In Kriging, the trend part of a prediction is called “the trend”. The fluctuation part is called “spatially-autocorrelated random error”. "Error" doesn't mean a mistake; it just means a fluctuation from the trend. "Random" means that the fluctuation (error) away from the trend is not known in advance, it could be up or down in elevation, it could be above or below the average climb of the stock market. "Spatially-autocorrelated" means that, while the fluctuations are not known exactly in advance, they have tendencies to be above the average or below the average together whenever they are in close proximity. This is positive spatial autocorrelation. It is also possible to have negative spatial correlation, where if one site is above the average, a nearby site tends to be below the average. Two assumptions are made about the spatially-autocorrelated random error. The first assumption is that it is 0 on average. In other words, some fluctuations will be on one side of the trend and some will be on the other side, but the differences, on average, will cancel each other out. The second assumption is that the autocorrelation of the error is purely spatial; it depends only on distance and not on any other property (such as position) of a location. This assumption is technically known as "stationarity."

Ordinary Kriging is done when one assumes there is no trend in the data, or, if there is one, it is weak enough that you can ignore it. Assuming that there is no trend in the data is mathematically equivalent to assuming that the data have a constant mean value. The points that make up the interpolated surface are the mean of all points in the search neighbourhoods.

Universal Kriging assumes there is a trend in the data, but the terms of the trend function are not known in advance. The data values are thought of as random errors that fluctuate around the unknown trend. The random errors are autocorrelated, meaning they tend to be above or below the trend in a way similar to their neighbours. The points that make up the interpolated surface are the mean of all points in the search neighbourhoods, plus the trend.

Kriging assumes that the distance or direction between sample points reflects a spatial correlation that can be used to explain variation in the surface. The Kriging tool fits a mathematical function to a specified number of points, or all points within a specified radius, to determine the output value for each location. Kriging is a multistep process; it includes exploratory statistical analysis of the data, variogram modeling, creating the surface, and (optionally) exploring a variance surface. Kriging is most appropriate when you know there is a spatially correlated distance or directional bias in the data. It is often used in soil science and geology.

Kriging is similar to IDW in that it weights the surrounding measured values to derive a prediction for an unmeasured location. The general formula for both interpolators is formed as a weighted sum of the data:

$$\hat{Z}(s_0) = \sum_{i=1}^{N} \lambda_i Z(s_i)$$

where:

$Z(s_i)$ = the measured value at the *i*th location

λ_i = an unknown weight for the measured value at the *i*th location

s_0 = the prediction location

N = the number of measured values

In IDW, the weight, λ_i, depends solely on the distance to the prediction location. However, with the kriging method, the weights are based not only on the distance between the measured points and the prediction location but also on the overall spatial arrangement of the measured points. To use the spatial arrangement in the weights, the spatial autocorrelation must be quantified. Thus, in ordinary kriging, the weight, λ_i, depends on a fitted model to the measured points, the distance to the prediction location, and the spatial relationships among the measured values around the prediction location. The following sections discuss how the general kriging formula is used to create a map of the prediction surface and a map of the accuracy of the predictions.

3.2.1.1. The variogram:

The spatial interpolation is a classic problem of estimation of a function F (x), where X = (x, y), in a point Xp of the plan from known values of F in a certain number, m, of surrounding points Xi:

$$F(x_p) = \sum_{i=1}^{m} W_i \cdot F(x_i) \quad (1)$$

The problem consists in determining the weighting, i.e. Wi, of each of the surrounding points. There are several manners to choose these weights. The two main known methods are the linear interpolation (according to the inverse of the distance IDW) and the method of the cubic splines (adjustment of cubic polynomials). Kriging chooses rather the weights from the degree of similarity between the values of F, i.e. from the covariance between points according to the distance between these points.

To make a prediction with the kriging interpolation method, two tasks are necessary:
- Uncover the dependency rules.
- Make the predictions.

To realize these two tasks, kriging goes through a two-step process:
- It creates the variograms and covariance functions to estimate the statistical dependence (called spatial autocorrelation) values that depend on the model of autocorrelation (fitting a model).
- It predicts the unknown values (making a prediction).

It is because of these two distinct tasks that it has been said that kriging uses the data twice: the first time to estimate the spatial autocorrelation of the data and the second to make the predictions.

Often, each pair of locations has a unique distance, and there are often many pairs of points. To plot all pairs quickly becomes unmanageable. Instead of plotting each pair, the pairs are grouped into lag bins. For example, compute the average semivariance for all pairs of points that are greater than 40 meters apart but less than 50 meters. The empirical semivariogram is a graph of the averaged semivariogram values on the y-axis and the distance (or lag) on the x-axis (see diagram below).

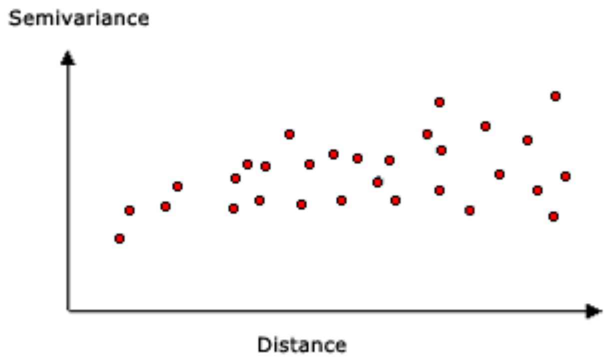

Example of diagram of empirical semivariogram

Spatial autocorrelation quantifies a basic principle of geography: things that are closer are more alike than things farther apart. Thus, pairs of locations that are closer (far left on the x-axis of the semivariogram cloud) should have more similar values (low on the y-axis of the semivariogram cloud). As pairs of locations become farther apart (moving to the right on the x-axis of the semivariogram cloud), they should become more dissimilar and have a higher squared difference (moving up on the y-axis of the semivariogram cloud).

3.2.1.2. Kriging Isoseismal line

Understanding a semivariogram—Range, sill, and nugget
As previously discussed, the semivariogram depicts the spatial autocorrelation of the measured sample points. Because of a basic principle of geography (things that are closer are more alike), measured points that are close will generally have a smaller difference squared than those farther apart. Once each pair of locations is plotted after being binned, a model is fit through them. Range, sill, and nugget are commonly used to describe these models.

Range and sill
When you look at the model of a semivariogram, you will notice that at a certain distance the model levels out. The distance where the model first flattens is known as the range. Sample locations separated by distances closer than the range are spatially autocorrelated, whereas locations farther apart than the range are not.

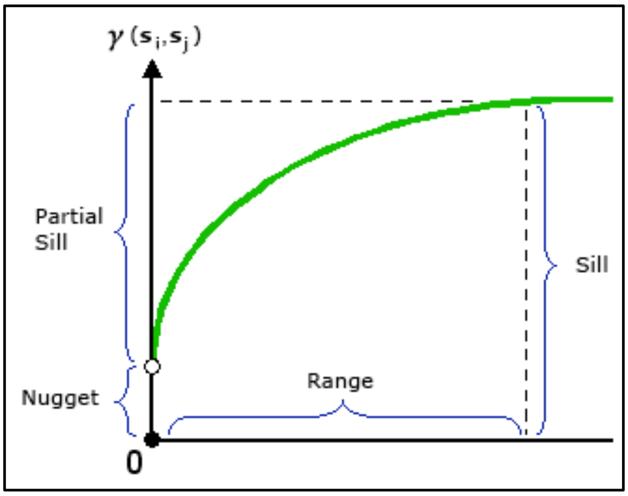

Illustration of Range, Sill, and Nugget components

The value at which the semivariogram model attains the range (the value on the y-axis) is called the sill. A partial sill is the sill minus the nugget. The nugget is described in the following section.

Nugget
Theoretically, at zero separation distance (for example, lag = 0), the semivariogram value is 0. However, at an infinitely small separation distance, the semivariogram often exhibits a nugget effect, which is a value greater than 0. If the semivariogram model intercepts the y-axis at 2, then the nugget is 2.
The nugget effect can be attributed to measurement errors or spatial sources of variation at distances smaller than the sampling interval (or both). Measurement error occurs because of the error inherent in measuring devices. Natural phenomena can vary spatially over a range of scales. Variation at microscales smaller than the sampling distances will appear as part of the nugget effect. Before collecting data, it is important to gain an understanding of the scales of spatial variation in which you are interested.

Like IDW interpolation, kriging forms weights from surrounding measured values to predict unmeasured locations. As with IDW interpolation, the measured values closest to the unmeasured locations have the most influence. However, the kriging weights for the surrounding measured points are more sophisticated than those of IDW. IDW uses a simple algorithm based on distance, but kriging weights come from a semivariogram that was developed by looking at the spatial nature of the data. To create a continuous surface of the phenomenon, predictions are made for each location, or cell centers, in the study area based on the semivariogram and the spatial arrangement of measured values that are nearby.

3.2.1.3. Example of an application to macroseismic data

De Rubeis et al (2005) demonstrate that kriging method is useful to produce interpolated intensity data at local and regional scale. (figure 7)

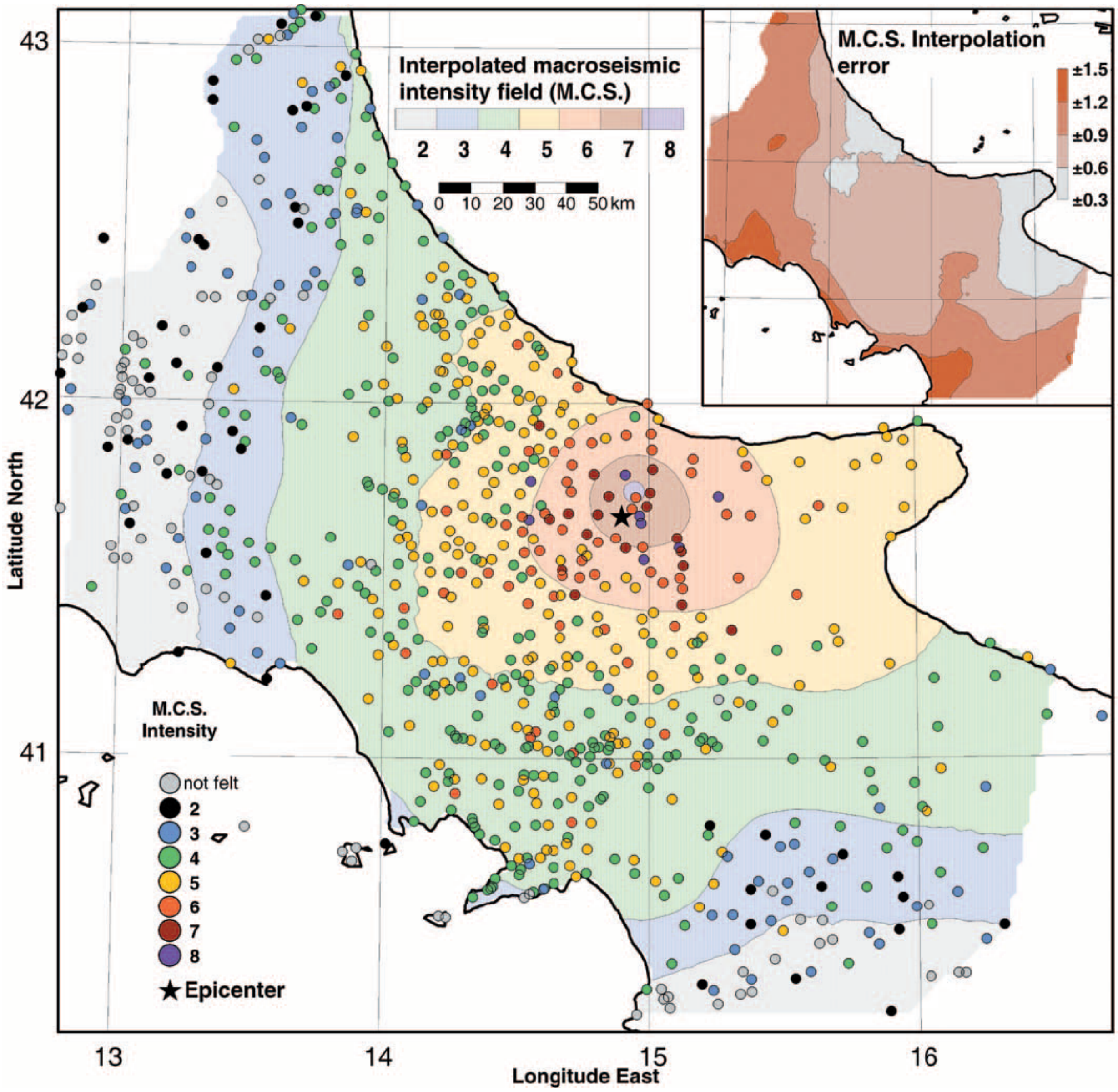

Figure 7 Macroseismic intensity data representation and field reconstruction of 31 October 2002, magnitude *M*L 5.4 earthquake. Original intensity values are drawn with colored circles (Mercalli-Cancani-Sieberg scale), the interpolated field is reproduced with shaded contours. Estimation error is displayed within the upper-right corner frame. (After De Rubeis et al. 2005)

4. Rambervillers data used for the methodological development.

In the first part of the work, we use the well-constrained Rambervillers earthquake (22 February 2003, Mw=4,8). It is the major event during the last decade in France.

We have for this event in our database 5212 intensities for the French territory.

Figure 8a shows the location of the data and the figure 8b the associated intensities values. The “circle” limit shape of the data is related to the limit of the survey done by the BCSF after this event. Notice that one department is empty at NW (Marne) as the prefecture did not accept to spread the form to municipalities of its department; therefore, no collective data were collected there. The other data, in Marne department and outside the circle, correspond to city for which we collected Individual forms filled on BCSF web site. The value affected to a city in that case is the mean of the SQI (single questionnaire intensity) deduced from the individual forms.
We see that the area defined by the BCSF for the official survey through prefecture, departmental administrative office, is of first importance. The individual forms are also important, in the first minutes, hours or even days when no collective forms are available or at places where not collective forms are collected, particularly for the felt maximum distance. Nevertheless, at distance where we collected only individual forms collected in 2003, the intensities are irregularly widespread.

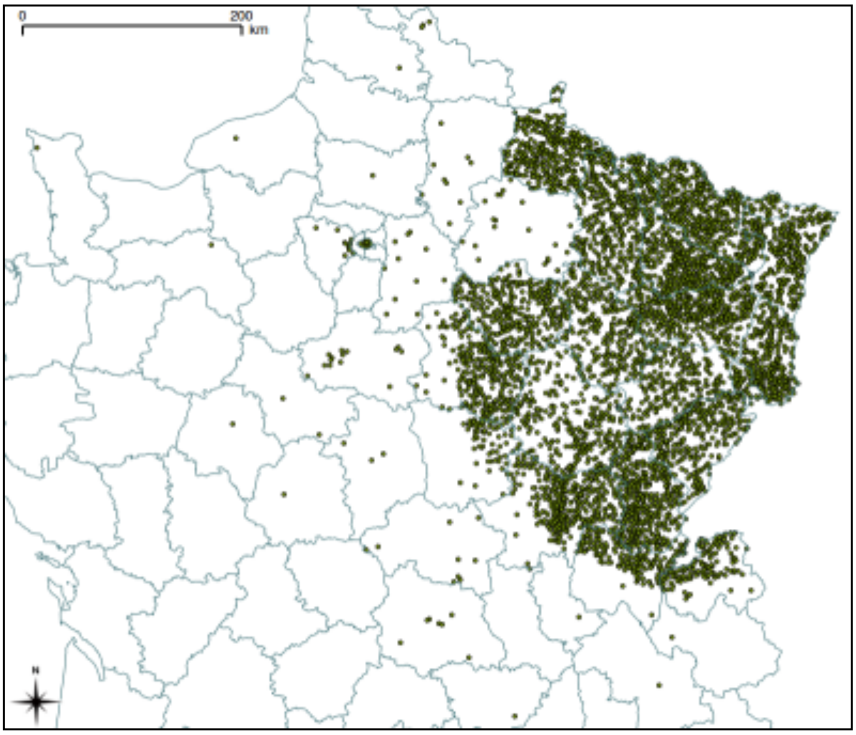

Figure 8a: Location of the cities where BCSF collected macroseismic data and where communal intensities have been estimated by BCSF for the Rambervillers earthquake, 22 February 2003,

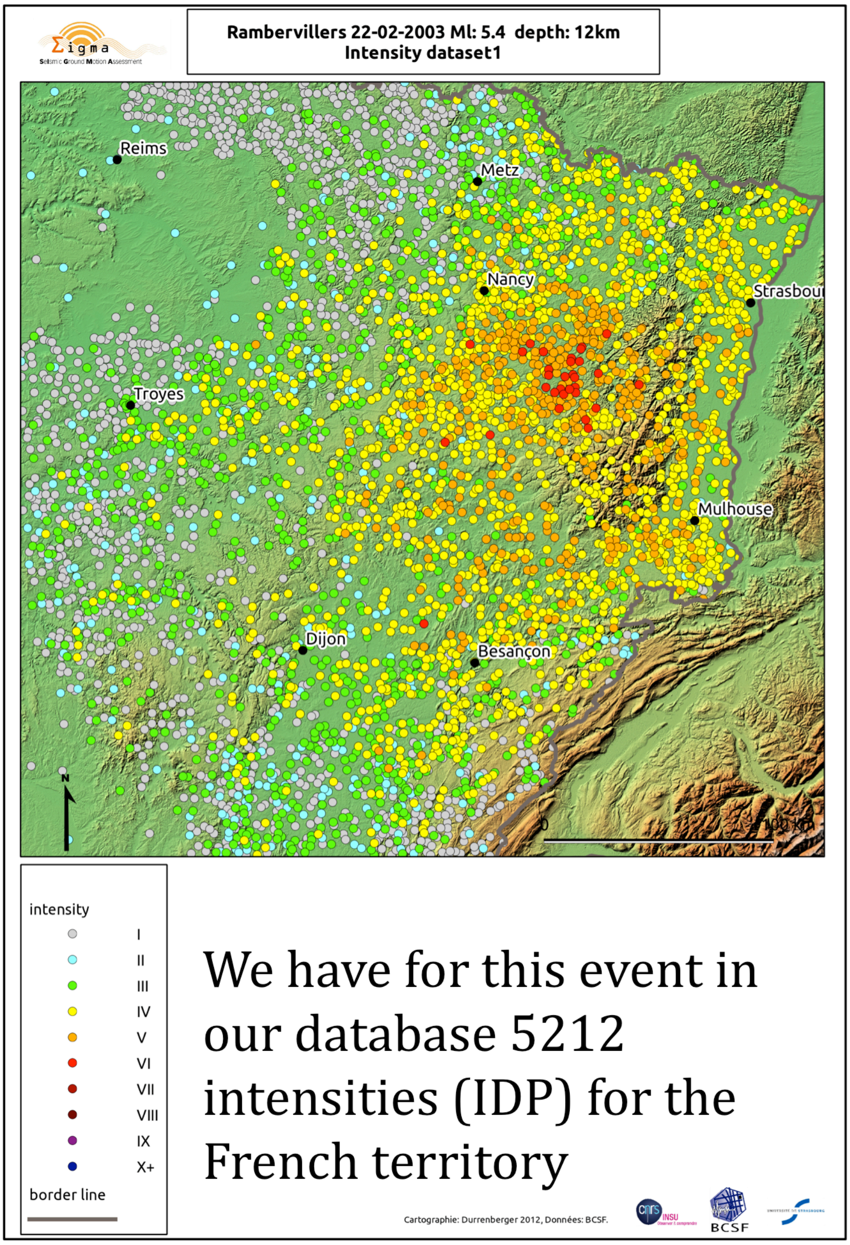

Figure 8a: Intensities collected and determined by the BCSF for the Rambervillers earthquake, 22 February 2003,

5. Rambervillers and Roulans earthquakes analysis:

5.1. Distribution analysis with the Voronoï diagram:

The first test on the data is to generate a quick set of cartographical representations to better understand the spatial distribution.

The decomposition of the space, with the help of the diagram of Voronoï, allows establishing a polygonization. Each polygon of this decomposition represents all the points of the plan that are the closest to a given point (of intensity). The value of this intensity is then associated with the whole polygon. It is a simple method, of classification of data. The decomposition for every point of intensity in the space allows representing quickly the spatial distribution and the density of the macroseismic intensity.

This decomposition confirms that the dataset (for the Rambervillers earthquake) is “uncompleted” in the east part (outside French territory) with high values at the NE border (figure 9). Therefore, the Voronoï diagram overvalues some intensity far from hypocenter. Moreover, the lack of intensity=I (not felt) does not allow reproducing, de facto, the limit of felt area.

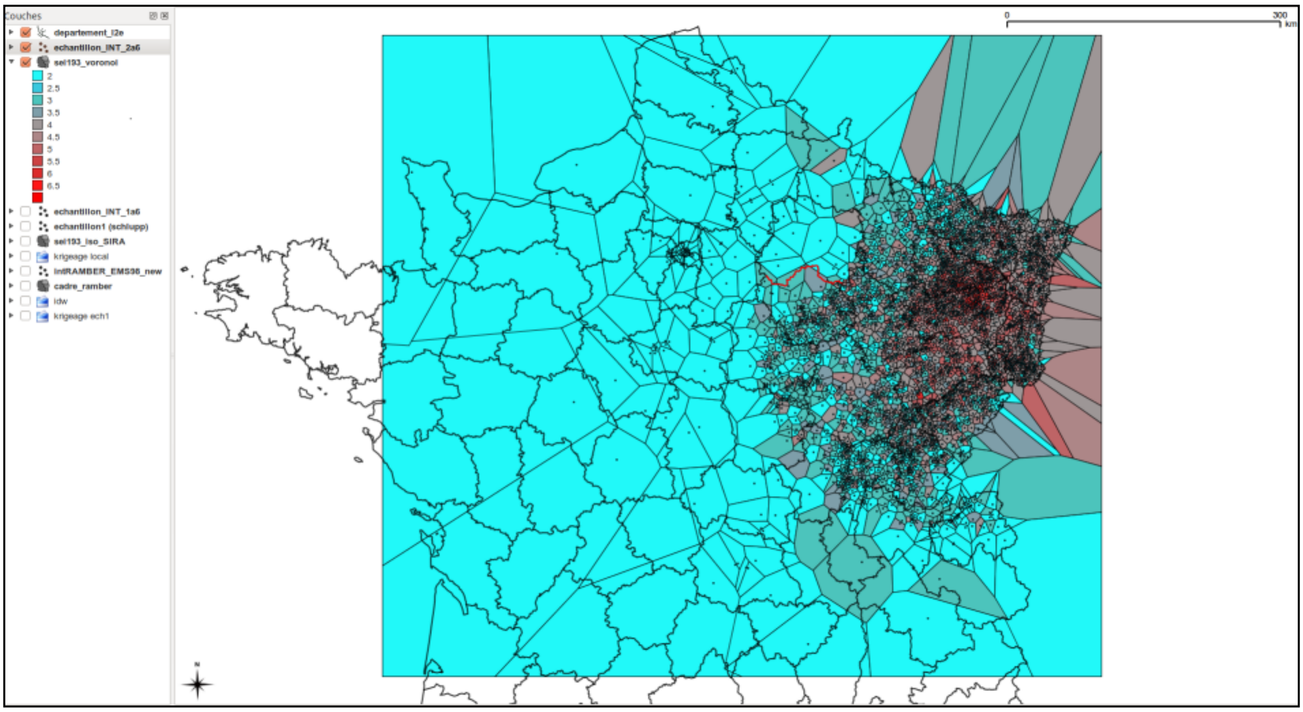

Figure 9: Voronoï diagram (Rambervillers earthquake, 02/22/2003)

<u>The Voronoï diagram has several advantages.</u>
- It reproduces integer values, which is the definition of intensity
- It does not calculate new value outside the dataset values
- It consider that the nearest observation is the best value, which is a good approximation for homogeneous area

- It shows clearly local variation of observed values inside the global trend.

<u>The main disadvantages for our purpose are</u>
- It consider that the nearest observation is the best value, which is a bad approximation for inhomogeneous area because it will widespread, over large area if the density of data is low, a local increase or decrease intensity. This variation can be due to any local or propagation effect or event due sometime to high uncertainty in intensity estimation
- It does not allow smoothing of the data.
- The total surface of the polygons with the same intensity is strongly related to the density of data. For example, few isolated points would contribute highly to the results, as the associated polygon will represent a large surface. We can see that in the Marne department, at the NW corner of the figure 10. Other example is the polygon built in Germany, where no data are available. They are dependent of local intensities in France, near the country border.

The density of data is therefore of high importance with the Voronoï approach. Finally, this method is not adapted to our aim.

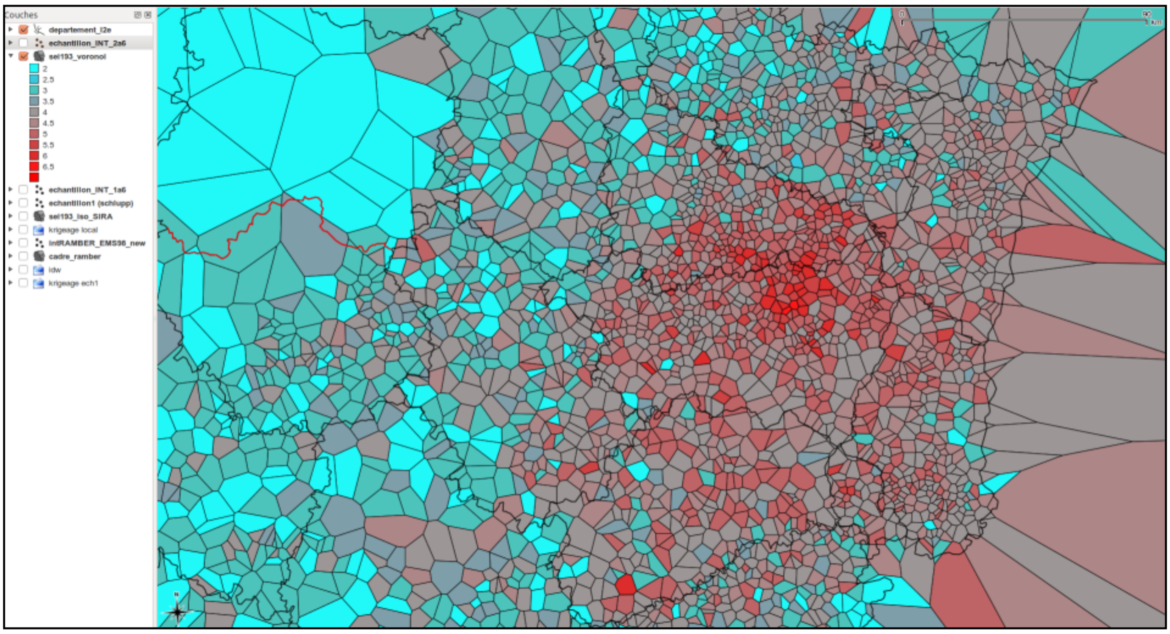

Figure 10: Voronoï zoom to hypocenter area (Rambervillers earthquake)

5.2. Reduction of Rambervillers dataset for robustness control:

The dataset of macrosismic intensities is very large for the earthquake of Rambervillers. There are more than 5200 points of observations. It corresponds to the scale of the data collected at the moment for an earthquake of intermediate magnitude in France. However, this density of information is not representative of available data for older earthquakes and the values of intensity I (not felt) are very rarely known for the past earthquakes. So, we simulated, for the earthquake of Rambervillers, a lower number of data and tested the impact on the procedure. The comparison of the results will give an estimation of the robustness of the procedure.

The dataset we will use for tests are:(cf table 1)

Dataset 1: contains all the observation stored in the BCSF database (data in France only) for the Rambervillers earthquake,

Dataset 2: contains the points of intensity higher or equal to II EMS98,

Dataset 3: contains a decrease of the observed points according to the intensity value

Dataset 4: is a step between dataset 2 and 3. It contains only intensity IV and higher considering that we loose other data (no reports)

The aim of the dataset 2 is to remove the intensity I, manly unknown. The aim of the dataset 3 is to simulate older event where we consider that intensity I and II are unknown, most of intensity III are not available, half of the intensity IV not determined. For VI to VII, we consider that most of the intensities are known as they are strongly felt and start to produce damage on weak buildings.

	Intensity EMS98	I	II	III	IV	V	VI	VII
Dataset1	% of data preserved	100%	100%	100%	100%	100%	100%	100%
Dataset2	% of data preserved	0%	100%	100%	100%	100%	100%	100%
Dataset3	% of data preserved	0%	0%	25%	50%	75%	90%	100%
Dataset4	% of data preserved	0%	0%	0%	100%	100%	100%	100%

Rambervillers earthquake: Dataset type	Number of observed points
Original dataset (dataset 1)	5212
EMS98 Intensity ≥ II dataset (dataset 2)	3494
Filtered EMS98 Intensity dataset (dataset 3)	1388

Table 1: Rambervillers earthquake datasets

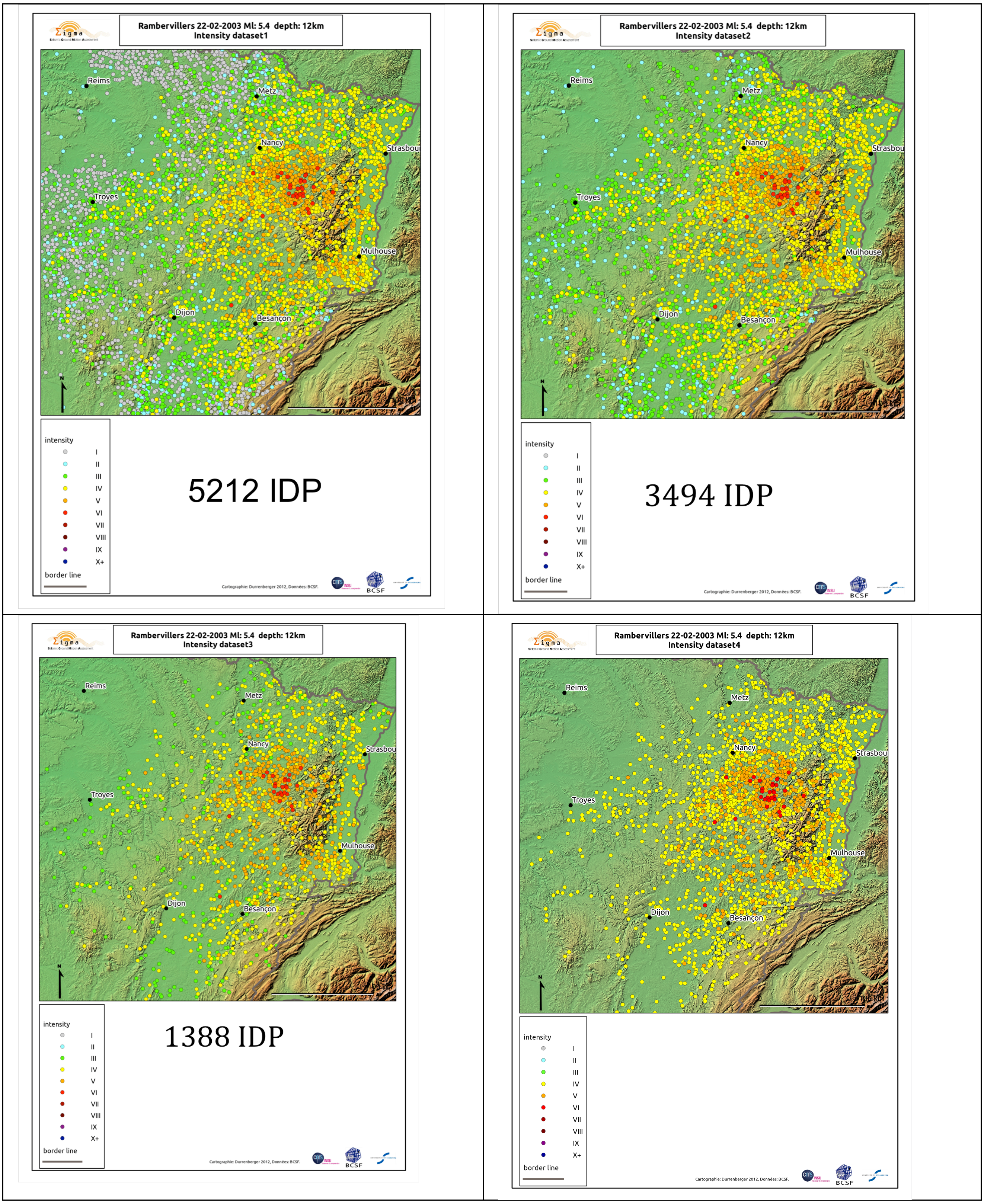

Figure 10b: Map of the Rambervillers earthquake datasets used in the study.

Despite this reduction of observed points, the dataset is still important (1388 points of observation). If we compare with the largest event in France during the last century, the Lambesc earthquake (magnitude around 6, June 9, 1909), they were « only » about 475 observations (Source : SisFrance web site, 2012) despite it is probably the best known historical event in France. We will, in a second step (not included in this report), decrease again the dataset of Rambervillers earthquake. The same procedure was applied on Roulans earthquake dataset.

5.3. Inverse distance weighted (IDW) interpolation method

The IDW interpolation method has two main advantages for us. The first, the results with this method keep the observed value at their place and the predicted value are dependent of the distance with observed intensity. The second is that the “expert draw” of isoseismal at BCSF uses the results of the IDW as a guide.

We will trace the isoseismals and compare the area in order to fit a result close to the original data and also similar to the manual tracing.
For this, we generate different interpolated grid for each dataset. The adjustable parameter is the weight attributed to each intensity point. Then isoseismal will be traced automatically. They will be compared to the original data and to the expert tracing (Cara et al. 2005).

The interpolation Inverse Distance Weighted (IDW) determines the values via the weighted combination of a set of points of sampling. The weighting is a function of opposite of the distance. The weighting used in the method IDW bases mainly on the opposite of the distance raised to a mathematical power. With the parameter "Power", we can control the influence of points known on the values interpolated according to the distance, which separates them. It is a positive and real number, the value of which by default is 2. The definition of a higher power allows imposing a stronger influence of the closest points. So, the surface will contain more details (will be less smooth) and the interpolated values approach more and more the value of the closest point. A value of less high power gives more influence to all the surrounding points, including the most remote, what generates a smoother surface.

The user has control over the mathematical form of the weighting function, the size of the neighbourhood (expressed as a radius or a number of points), in addition to other options.

Weighting function:
The simplest weighting function is inverse power:
w(d)= 1/dp

with p>0. The user specifies the value of p. The most common choice is p= 2. For p= 1, the interpolated function is "cone-like" in the vicinity of the data points, where it is not differentiable.

Because the formula IDW is not connected to a real physical process, there is no means to know what is the value of optimal power. Generally speaking, an important power must be used with caution. Also let us not forget that if the distances are big or if the value of power is high, prediction on remote points can be aberrant.

The choice and the control of this value will be made on the basis of the graphic results, which present surfaces by dataset and by type of interpolation according to the degree of weighting. After diverse initial tests, we concentrate on the degrees of weighting from 1 to 4.

5.3.1.1. Preliminary results with IDW method on Rambervillers earthquake.

Notice that we present here under preliminary results and they have to be considered, at this step, as guide for discussion and improvement of the procedure.

First we show the resulting images produced by the various datasets of Rambervillers earthquake. For each figures, we plot the “expert” isoseismal (Cara et al. 2005) in black bold line over the results of the process.

Dataset1	
Figure 11: Isoseismal lines from IDW P2	Figure 12: Isoseismal lines from IDW P3
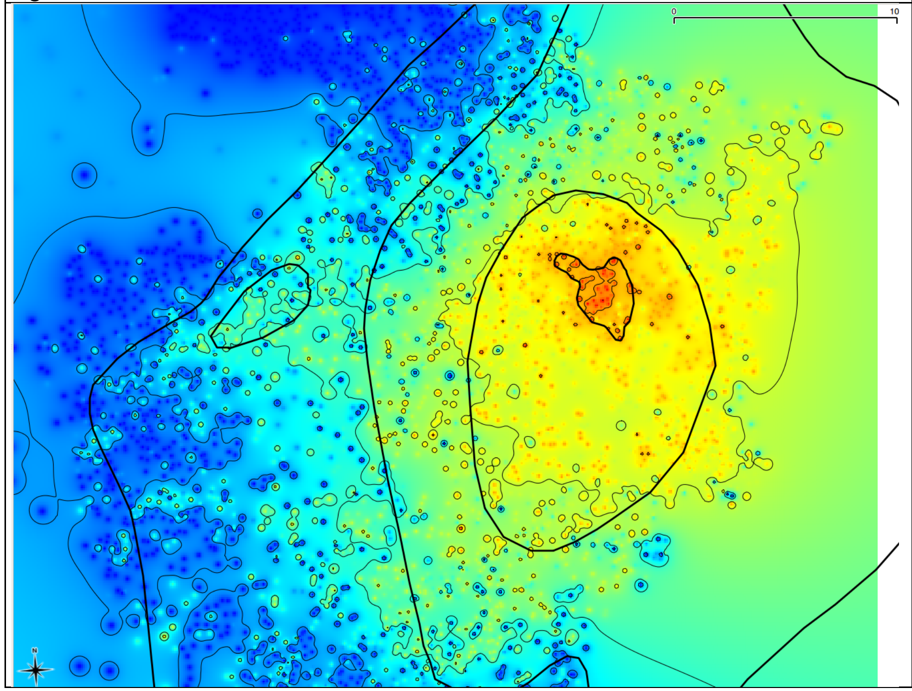	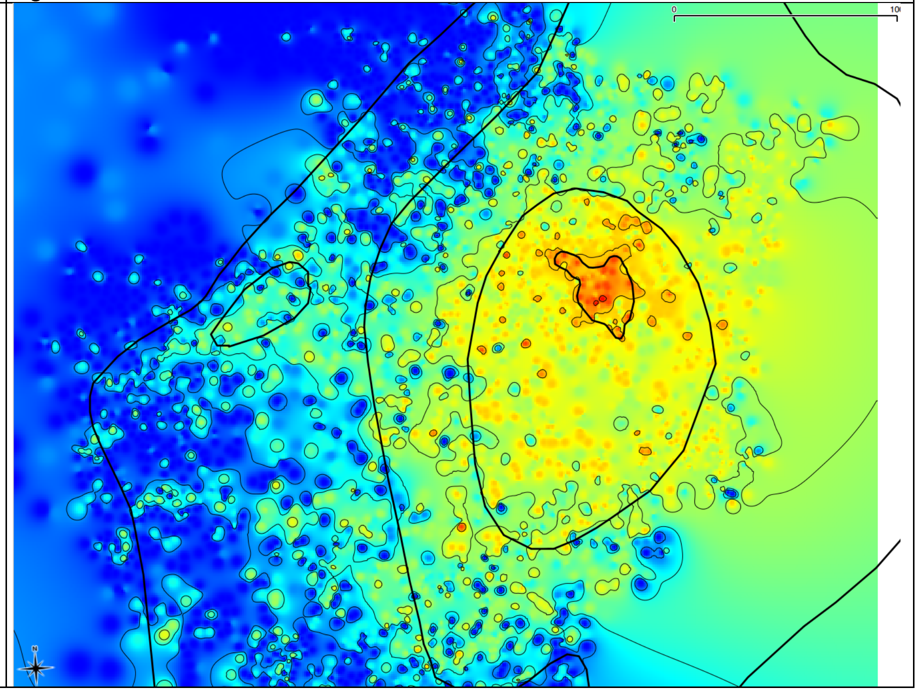

Black bold lines over the results of the process are the plots of the “expert” isoseismal (Cara et al. 2005).

Dataset2	
Figure 13: Isoseismal lines from IDW P2	Figure 14: Isoseismal lines from IDW P3
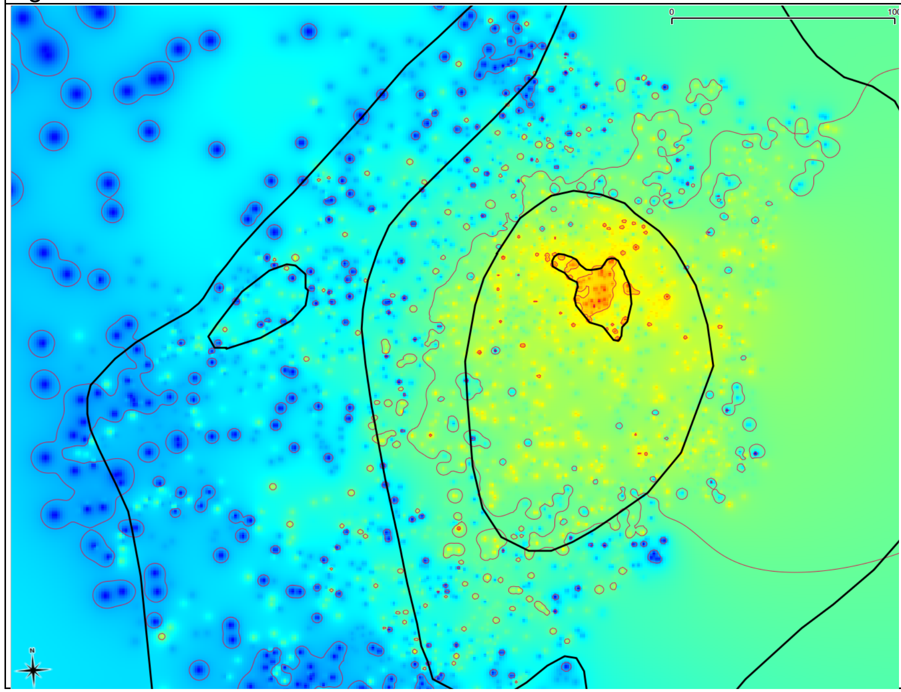	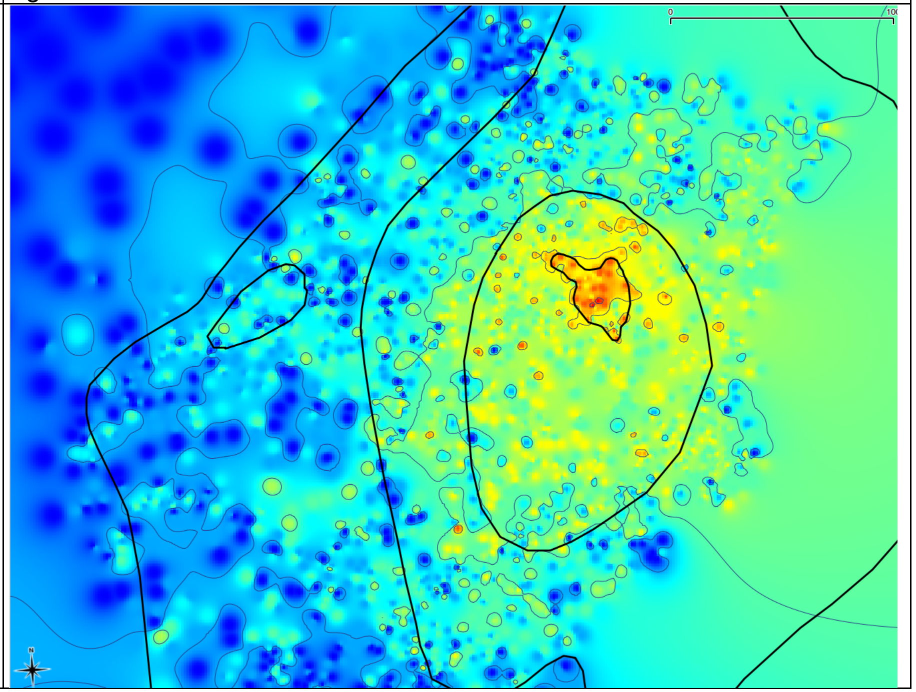

Black bold lines over the results of the process are the plots of the “expert” isoseismal (Cara et al. 2005).

Dataset3	
Figure 15: Isoseismal lines from IDW P2	Figure 16: Isoseismal lines from IDW P3
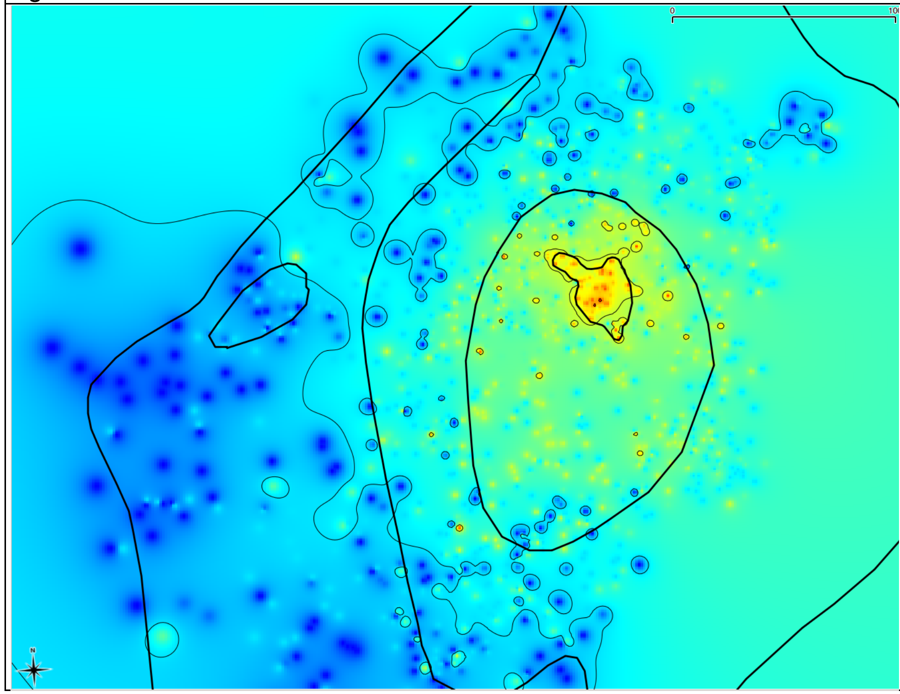	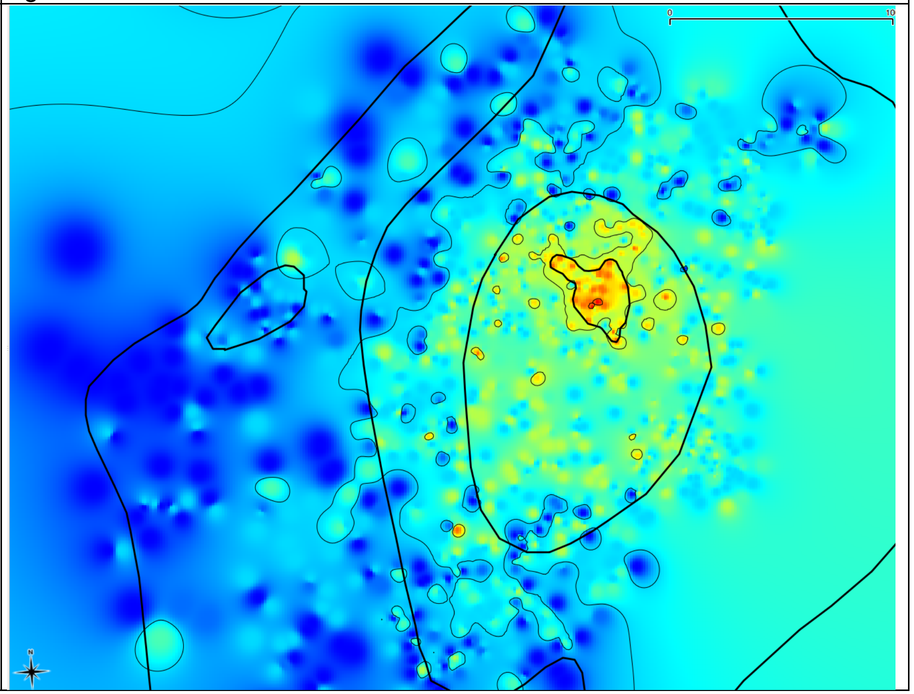

Black bold lines over the results of the process are the plots of the "expert" isoseismal (Cara et al. 2005).

The diagrams below show the area for each weighting Degree, from 1 to 4 of the inverse distance weighted interpolation and for the various datasets.

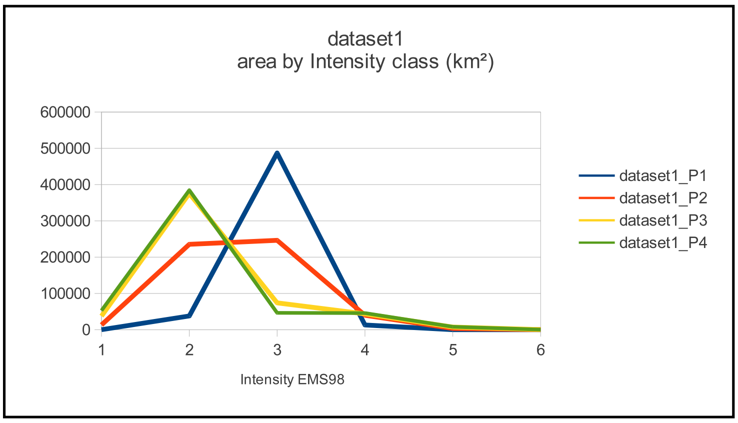

Figure 17: The surface of each intensity is presented in km² for one degree of weighting. For example, dataset1_P1 is the dataset1 (full data) and for IDW with a weighting of degree 1.

For the dataset1 (figure 17), we observe that the surfaces versus intensity are similar for the degree 3 and 4. But they are strong differences between the degree 1, 2 and 3-4.

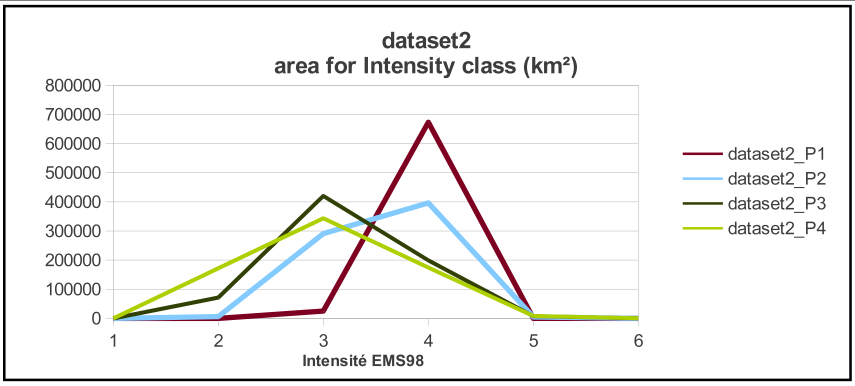

Figure 18: The surface of each intensity is presented in km² for one degree of weighting. For example, dataset2_P1 is the dataset2 (full data without Intensity I) and for IDW with a weighting of degree 1.

For the dataset2 (figure 18), we observe that the surfaces versus intensity are again similar for the degree 3 and 4. But they are again strong differences between the degree 1, 2 and 3-4.

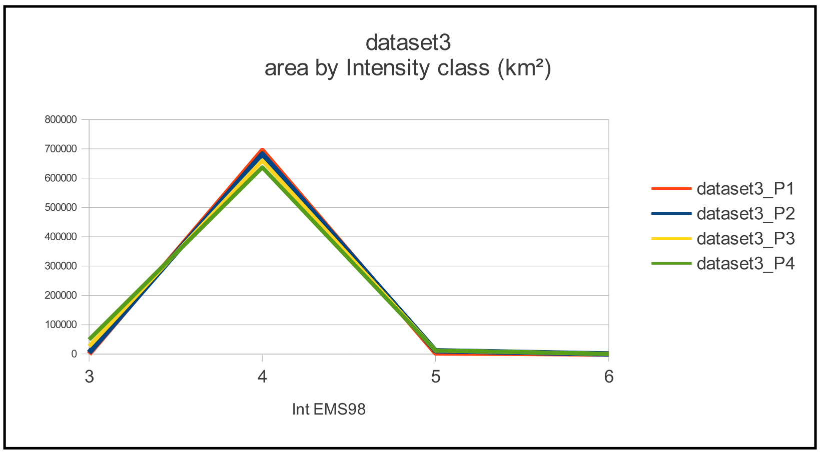

Figure 19: The surface of each intensity is presented in km² for one degree of weighting. For example, dataset3_P1 is the dataset3 (reduced dataset I) and for IDW with a weighting of degree 1.

For the dataset3 (figure 19), we observe that the surfaces versus intensity are similar for the degree 1, 2, 3 and 4.

Then, if we plot the results of the three datasets and weighting values (figure 20) on the same graph, we observe their impact on the results.

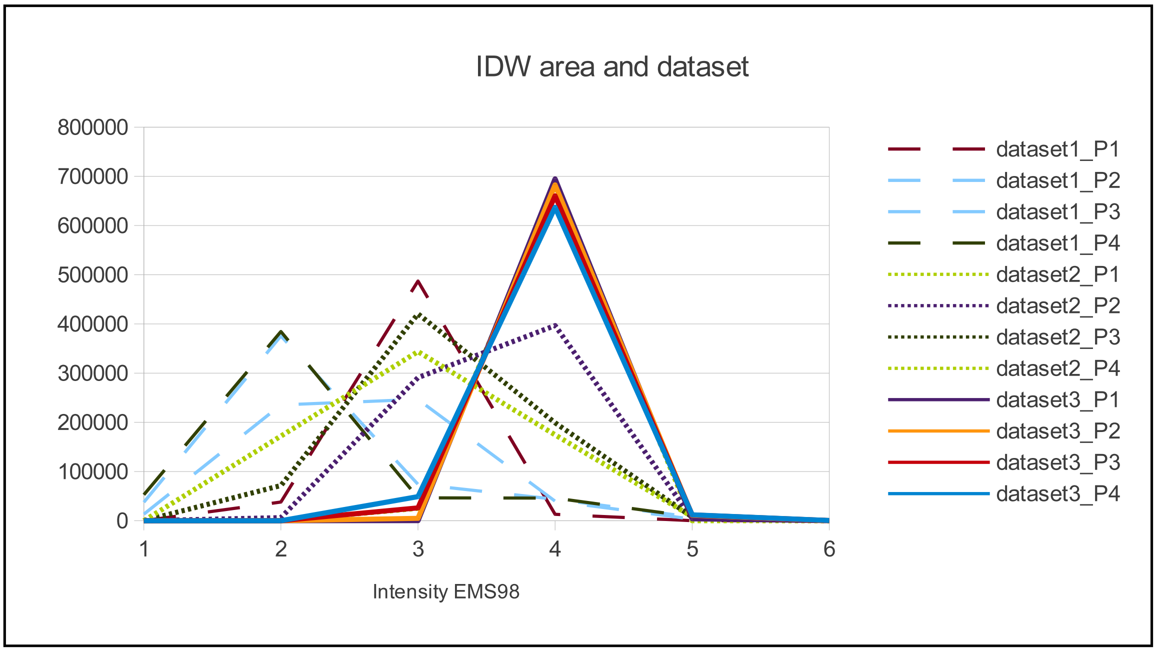

Figure 20: plot of the intensity area deduced from IDW method for the 3 datasets and the weighting of 1 to 4.

We see that the intensity surfaces vary a lot using different dataset for the same earthquake; therefore the IDW method is not robust one for automatic analysis at this step of the study.

5.3.1.2. Preliminary results with IDW method on Roulans earthquake.

Notice that we present here under preliminary results and they have to be considered, at this step, as guide for discussion and improvement of the procedure.

We show the resulting images produced by the various datasets of Roulans earthquake.

Dataset2	
Figure 21: Isoseismal lines from IDW P2	Figure 22: Isoseismal lines from IDW P3
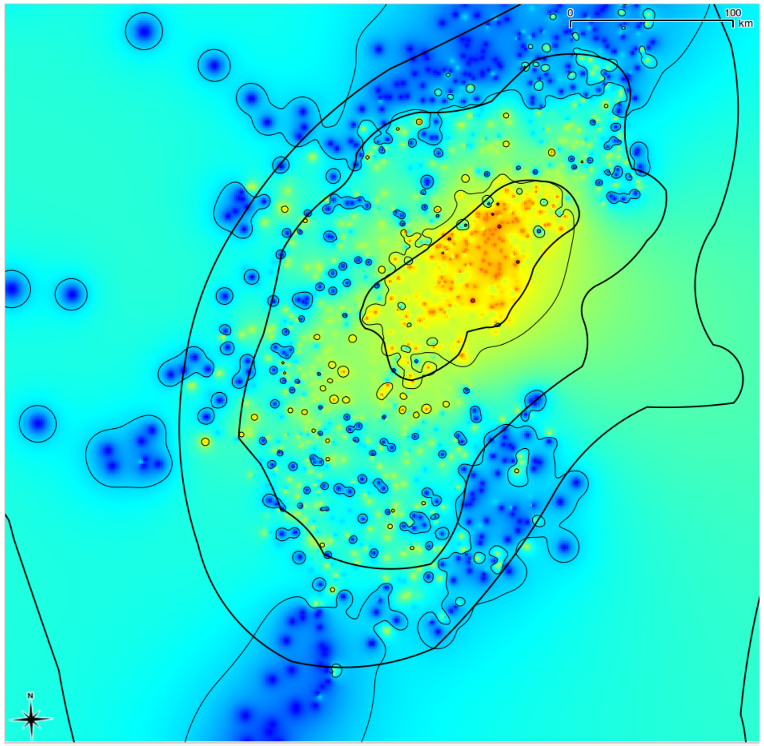	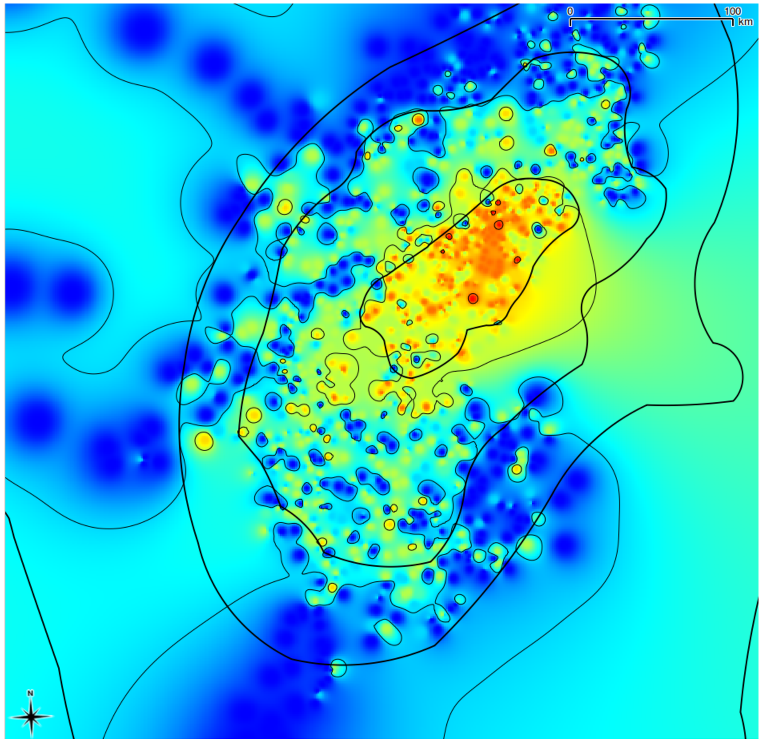

Black bold lines over the results of the process are the plots of the BCSF “expert” isoseismal (Cara et al. 2007).

Dataset3

Figure 23: Isoseismal lines from IDW P2

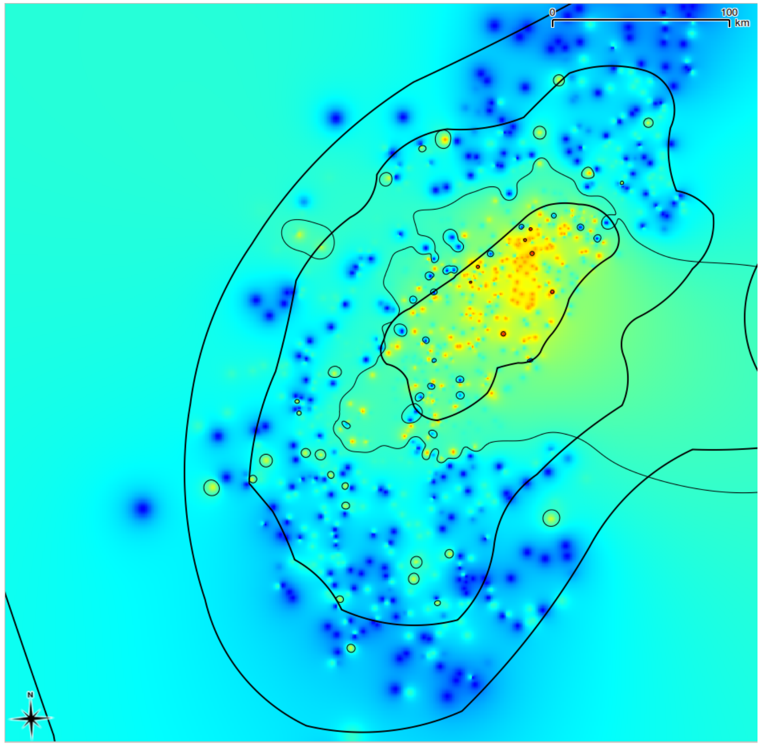

Figure 24: Isoseismal lines from IDW P3

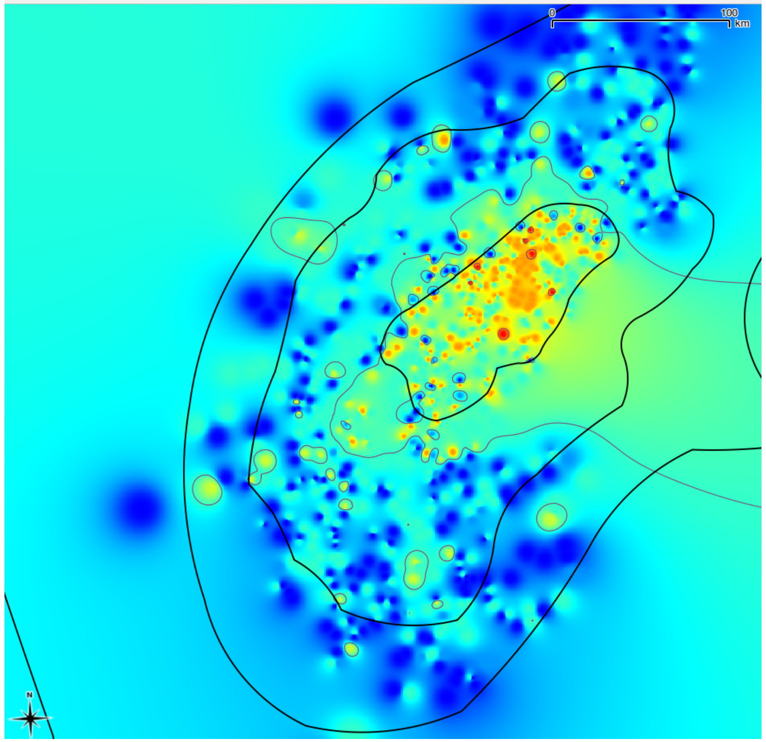

Black bold lines over the results of the process are the plots of the BCSF “expert” isoseismal (Cara et al. 2007).

5.4. Kriging method

5.4.1. Kriging Isoseismal line

We will test the universal kriging method on the 4 datasets with an interpolation of 0,1 in Intensity to better follow the decrease of the intensity in the epicentral area. The universal kriging method is applied successively; the estimation (theoretical variogram) is never inferior to the range of the original variogram.

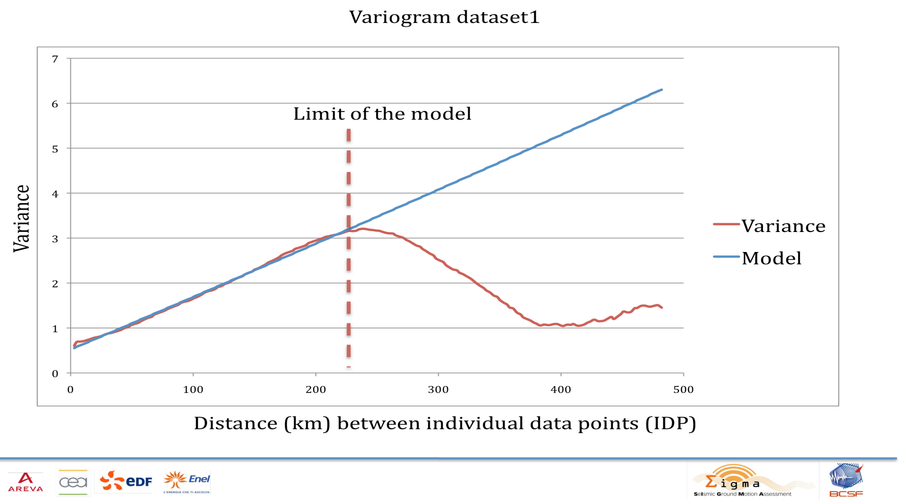

Figure 26: Rambervillers Earthquake variogram (dataset1):

We applied the kriging method on the data following the schema her under.

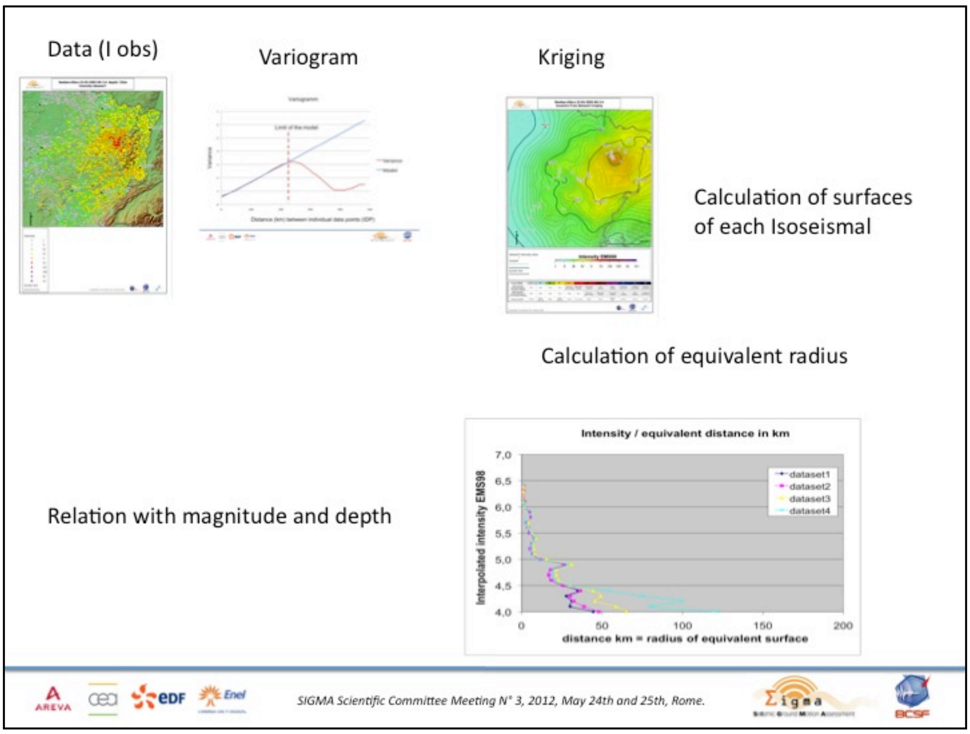

Figure 27: Schema of the kriging method until area estimation

We compare the result to the initial data and we observe a general trend in the difference between Intensity calculated with the kriging method and the intensity observed. This id done to see how far are the kriging results from the original data and then give a first statistical approach on the reliability of the method at this step of the study. We observe that the low intensities are overestimated and the highest intensity are underestimated.

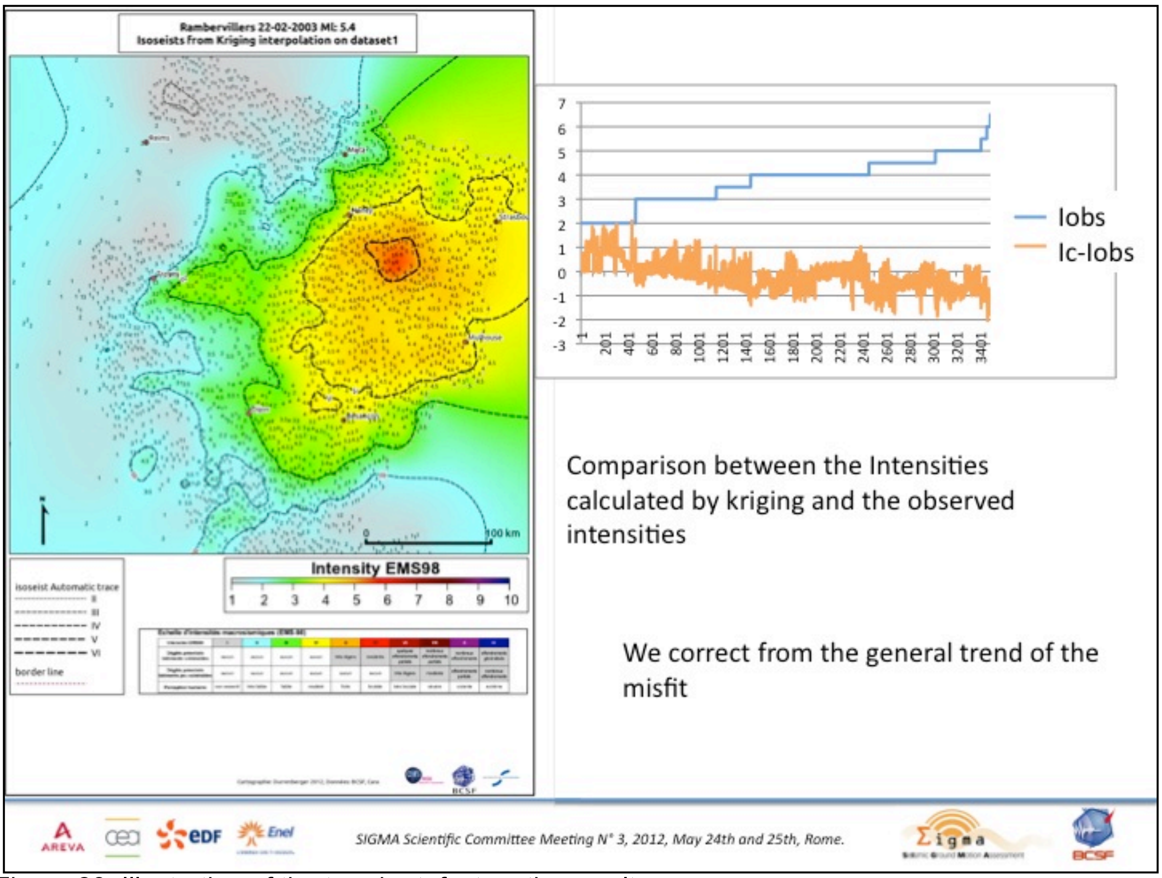

Figure 28: Illustration of the trend artefact on the results.

Therefore, we introduced a correction of this tendency and include it in the procedure.

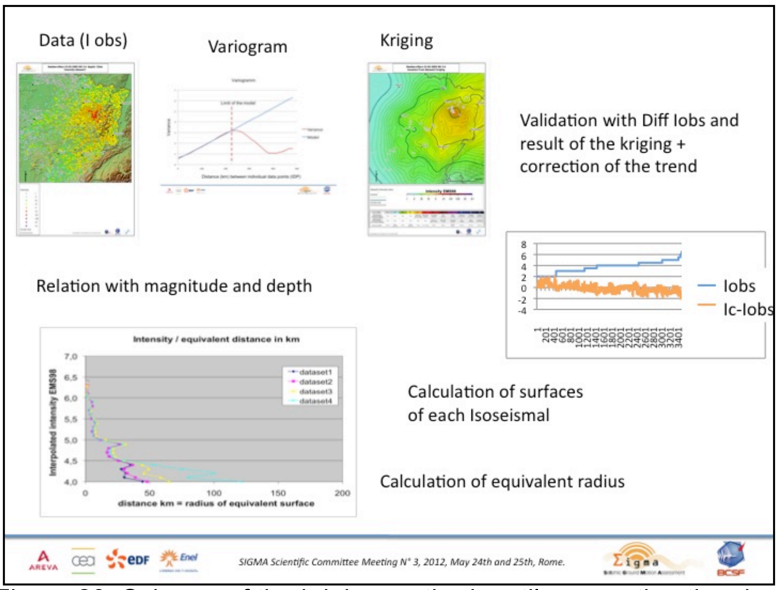

Figure 29: Schema of the kriging method, until area estimation, including the tendency correction

The kriging method applied on dataset1:

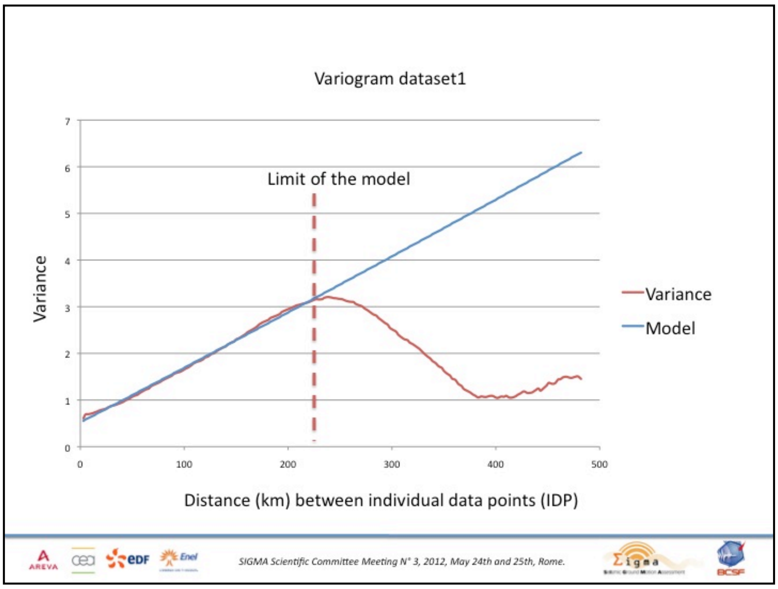

Figure 30: Variogram for dataset1

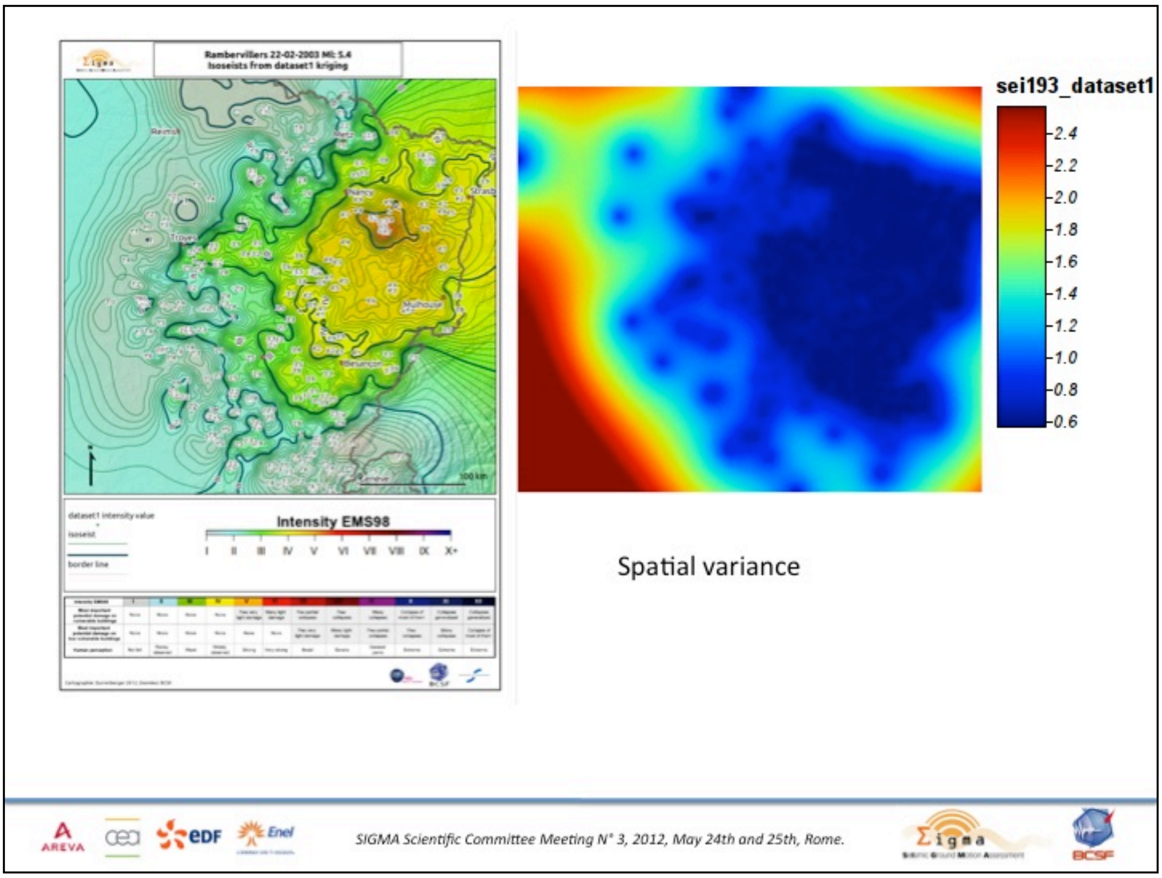

Figure 31: Isoseismal lines and spatial variance from Kriging adjusted for dataset1

<u>The kriging method applied on dataset2 :</u>
The theoretical variogram is not equal to the dataset1 variogram, but the method is the same: after calculating a theoretical variogram fitted to the variance, we can interpolate the intensity values.

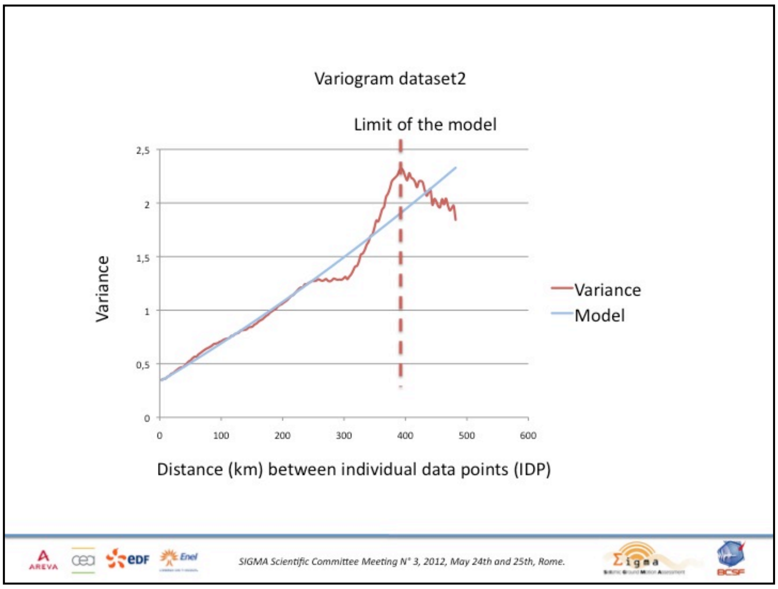

Figure 32: Variogram for dataset2

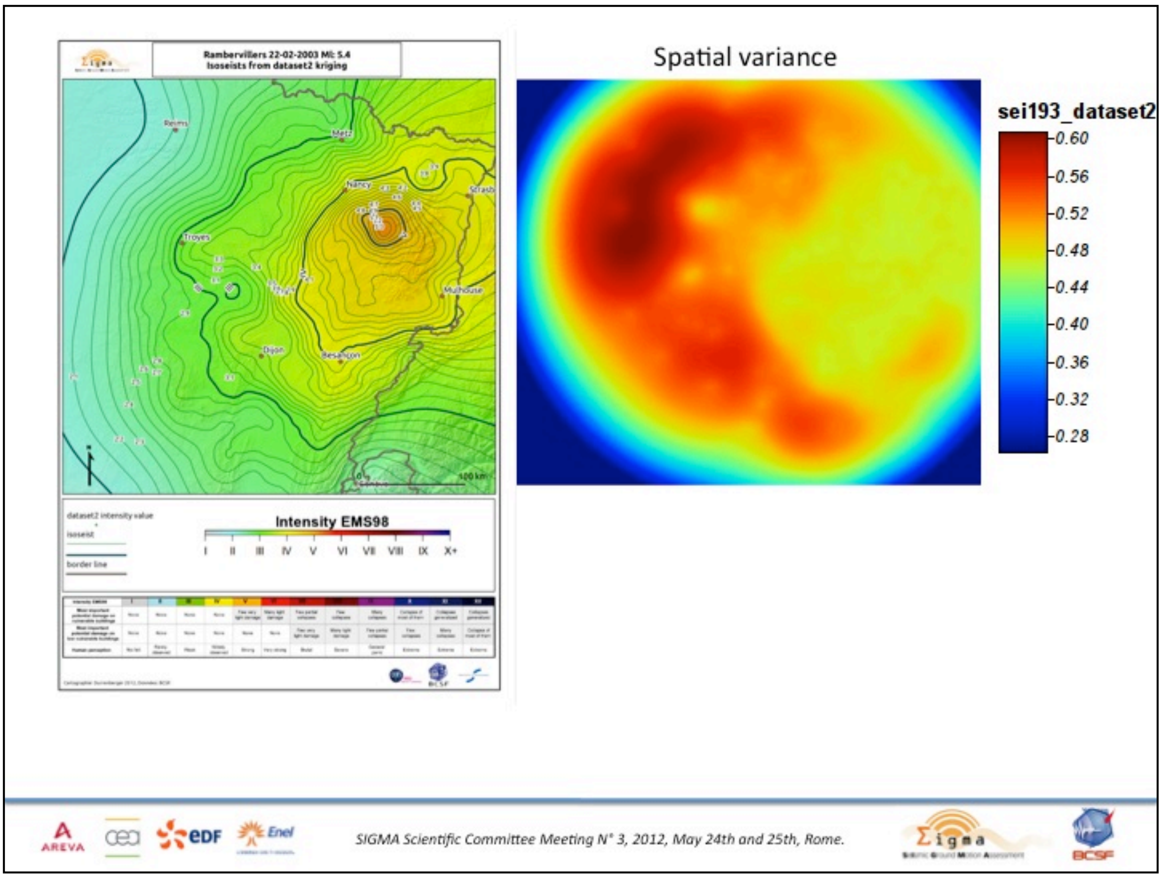

Figure 33: Isoseismal lines and spatial variance from Kriging adjusted for dataset2

<u>Kriging model applied to dataset3 (filtered):</u>
We suppose that the method will produce a smoother result for low intensities due to the lack of original data, but also similar intensity delimitation for high values of the sample. As we can see in the figure 35, the insulated spot is not present any more. The isosmeismals lines are smoother than the other interpolation.

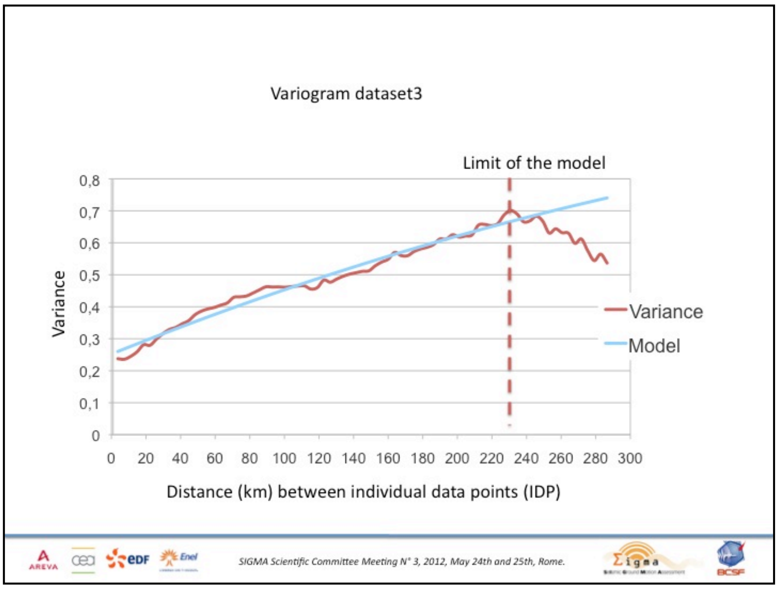

Figure 34: Variogram for dataset3

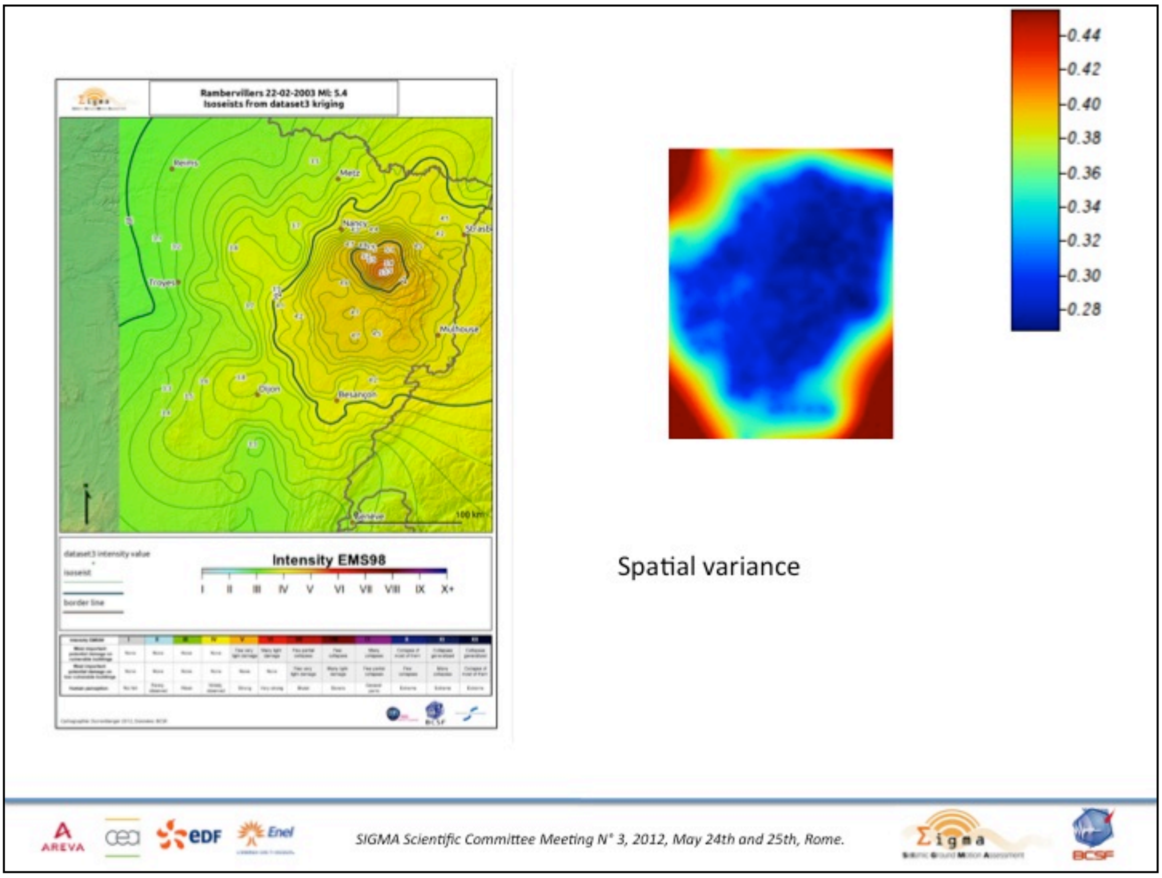

Figure 35: Isoseismal lines and spatial variance from Kriging adjusted for dataset3

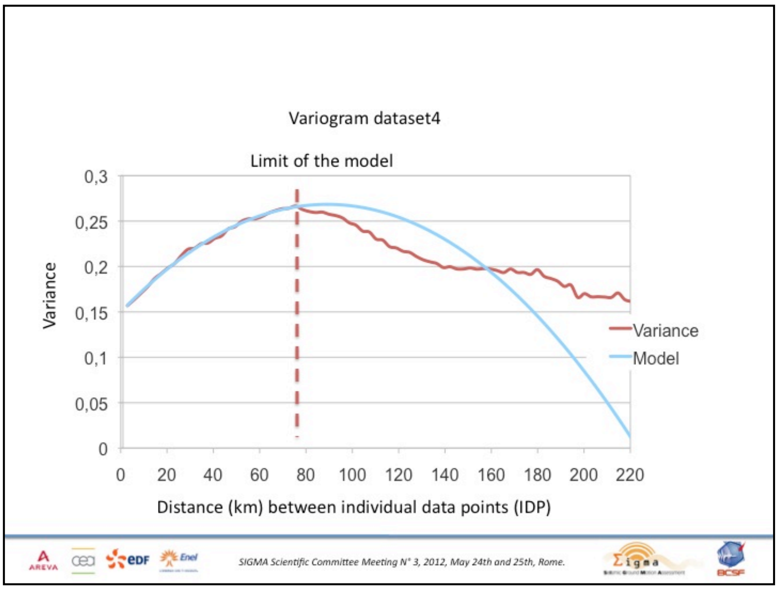

Figure 36: Variogram for dataset4

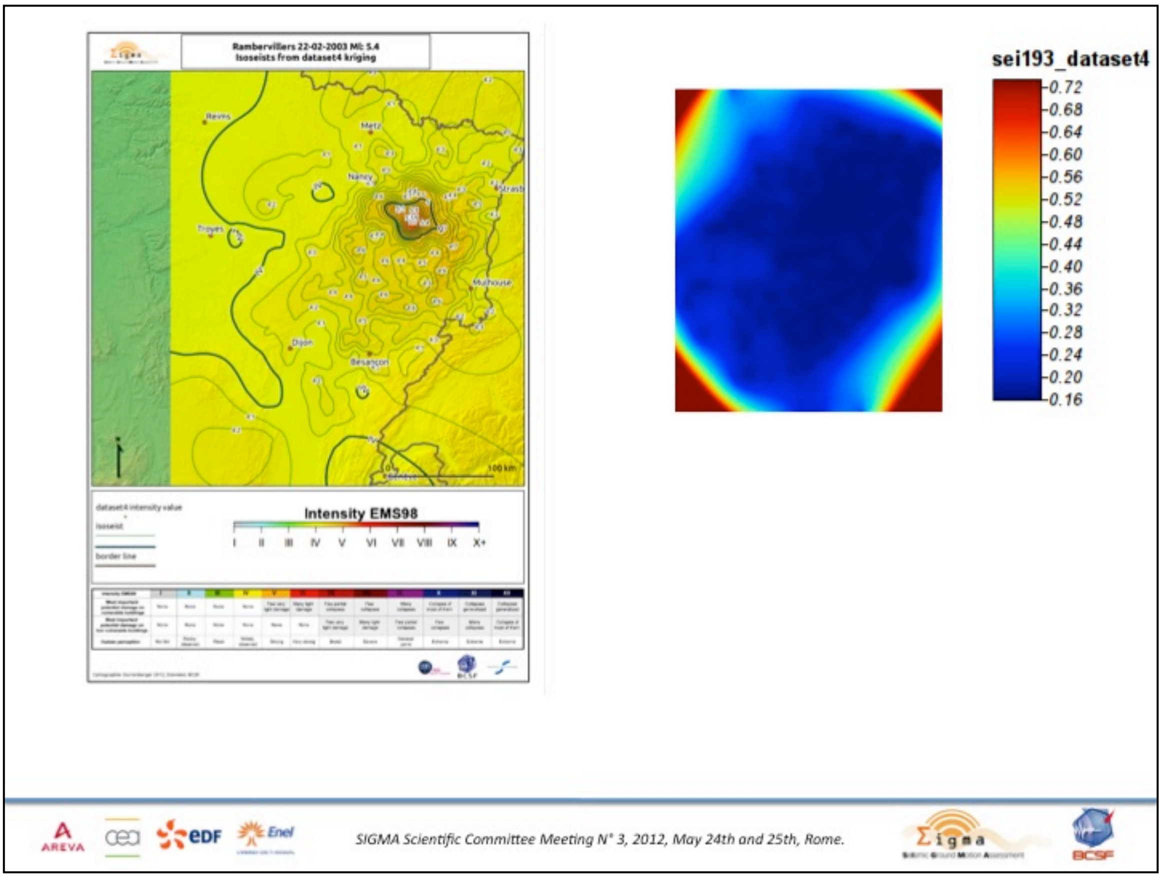

Figure 37: Isoseismal lines and spatial variance from Kriging adjusted for dataset4

5.4.2. Preliminary results with Kriging method on Rambervillers earthquake.

Notice that we present here under preliminary results and they have to be considered, at this step, as guide for discussion and improvement of the procedure.

First we show the resulting images produced by the various datasets of Rambervillers earthquake.

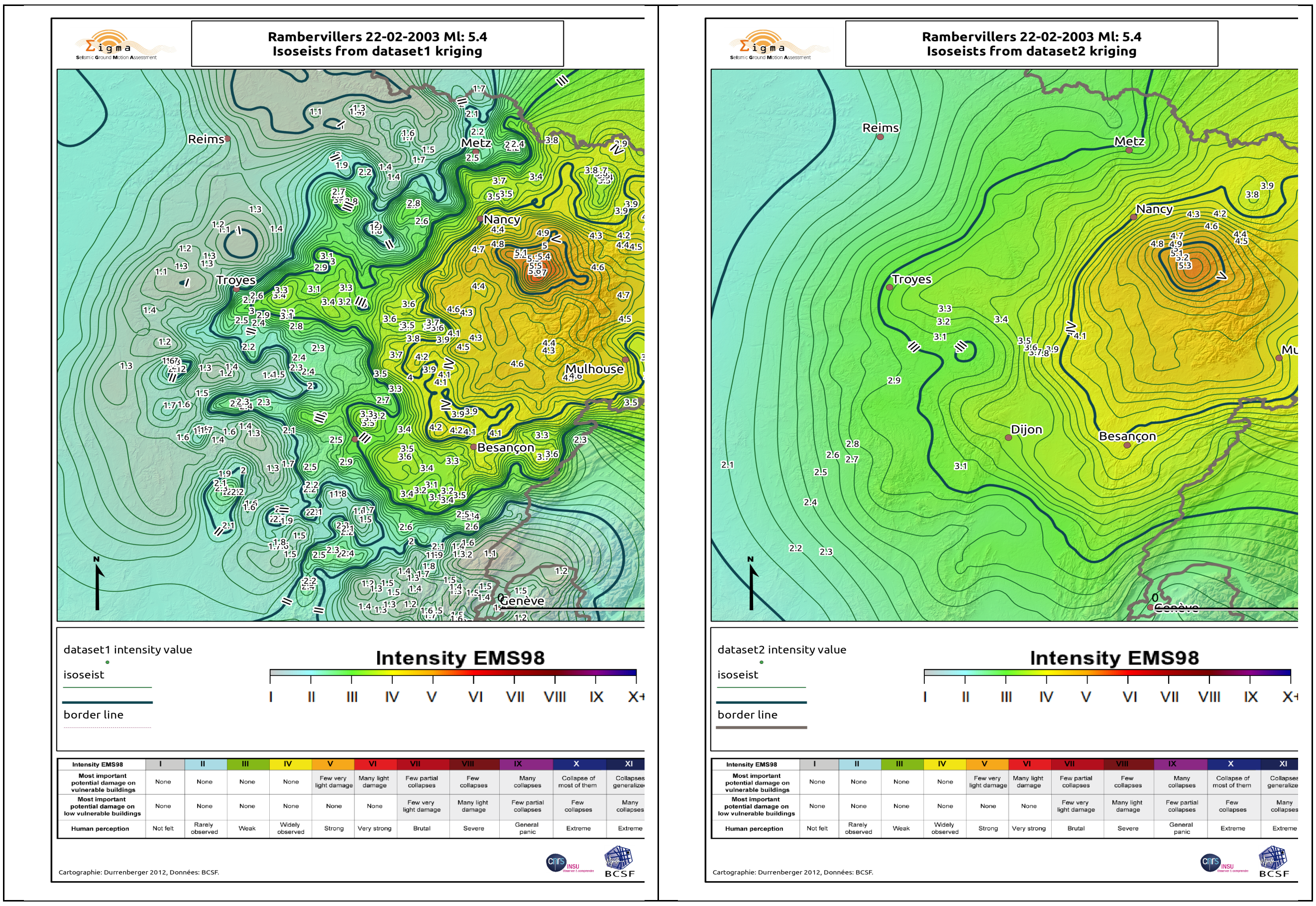

Figure 38: isoseismal following kriging method for datasets 1 and 2.

5.4.3. Comparison between the results of the 4 datasets

We describe the isoseismal area for each class of intensity by each type of dataset for Rambervillers earthquake. To better illustrate the evolution of the isoseismal area, we convert the surface of each isoseismal to an equivalent circle (same area) and we plot the radius of the circle versus intensity. We call it "equivalent circle radius". As we can see in the figure 40, the impact for equivalent circle radius less than 20 km is very low. Nevertheless, we can ses on figure 39, for a dataset4 that the isoline less than 4,4 are interrupted by the contry border and are then not contrained. It will be necessary to include a correction for this data lost that can happened for event near shore line. This will be studied in the nest step of the study.

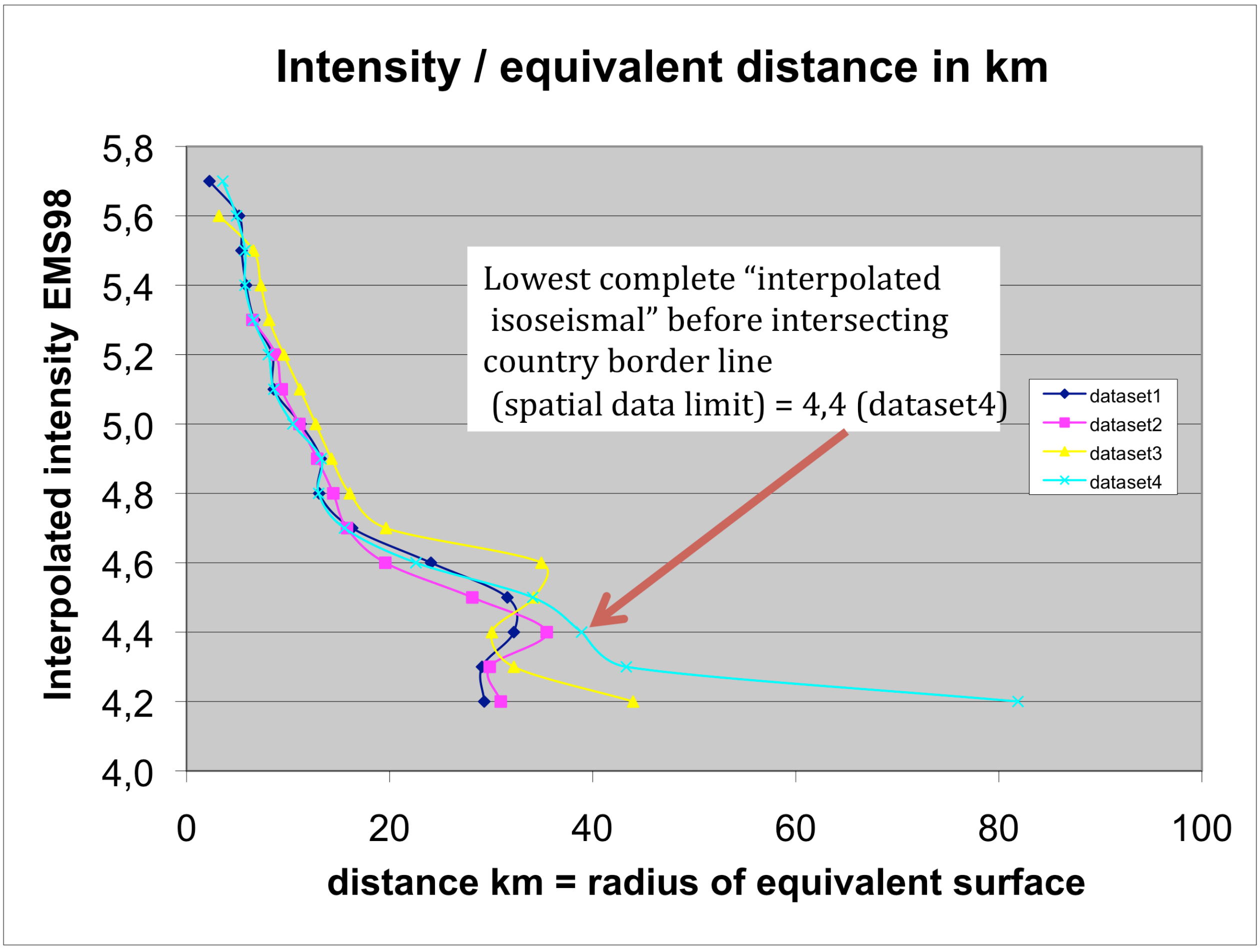

Figure 40: comparison of isoseismal area for each datasets using equivalent circle radius (non cumulated "equivalent circle radius" at X axis).

6. Conclusions

Conclusions

-The method based on isoseismal area has been

- -Advantage:
  - - no need to locate the epicenter,
  - - not dependent to the knowledge of Io,
  - - not sensitive to "elongated" isoseismals
- -Disadvantage:
  - - need to trace "objectively" isoseismal and solve associated pb

-IDW is very sensitive to local variation of IDP

- kriging gives a good estimated for the isoseismal mapping for the highest intensities

- We use an equivalent radius (distance) for the isoseismals area

Next step of the study

- Test the stability of the results with stronger decrease of data (Rambervillers)

- Introduction of correction due to partial isoseismal (limit by border line or shore line) => quality class for the results.

- Apply on Roulans earthquake (area/Intensity)

- Apply on well know event until 1905 (using data from Sisfrance + results from magnitude depth estimation from SI-Hex project)

- Establish a relation between the I-extrapolated and slope (determined on the plot of equivalent distance versus intensity) with magnitude-depth parameters for France.

7. Annexe

7.1. General scheme of the procedure

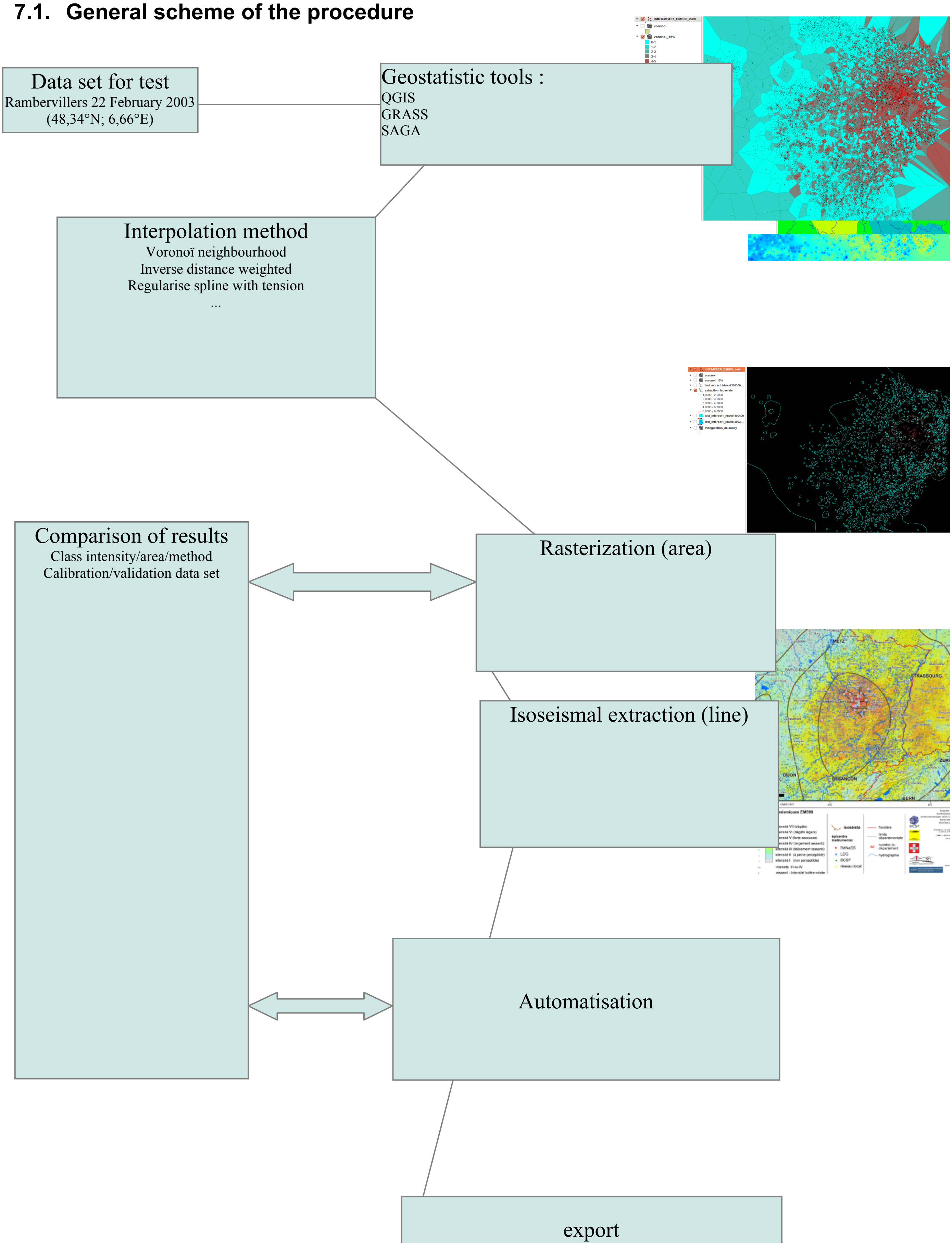

7.2. Comparison between 2 methods, Kriging and "expert interpolation" for Roulans earthquake:

The IDW and kriging methods are applied on different dataset type and events.

<u>Roulans earthquake:</u>
With a not adjusted variogram, does mean which is not based on the maximum range (the range which corresponds at the top of the graph below), we have results badly estimated. Beyond the summit of the variogram, the autocorrelation decreases. The interpolation and the isoseismals do not correspond to isoseismals interpreted manually.

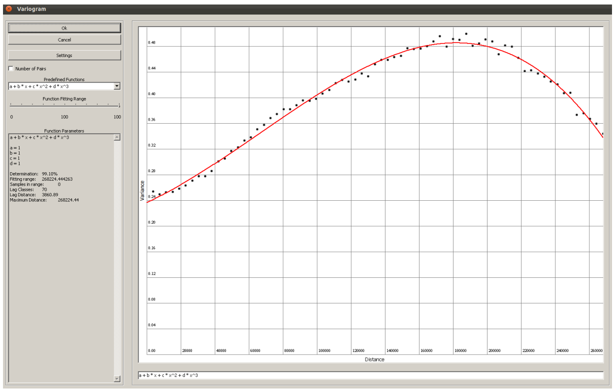

Figure 38: Variogram of dataset3 not adjusted:
T pa

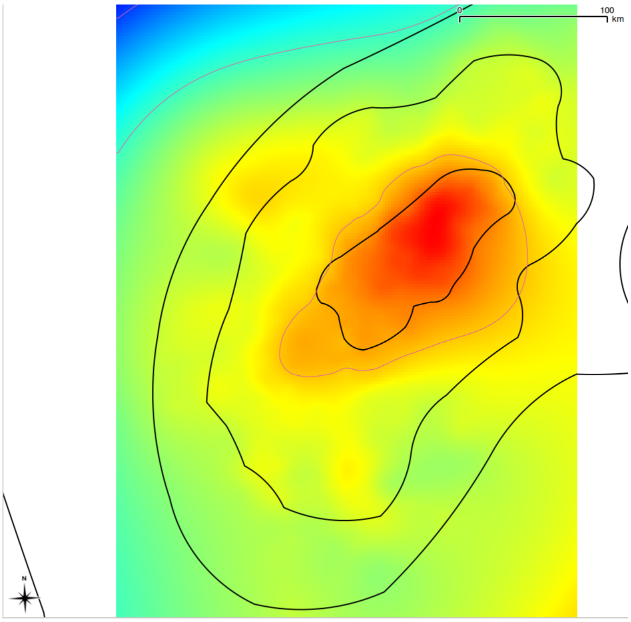

Figure 39: Isoseismal corresponding to the varigram not adjusted of dataset3

The generated isoseismals is not in agreement with the isoseismal of manual draw. Indeed the isoseismal of value V (thick black line) around the red orange zone is close to the isoseismal of value IV (grey and fine line) stemming from the kriging; there is thus an adjustment to be made on the summit of the variogram which corresponds at the beginning of autocorrelation.

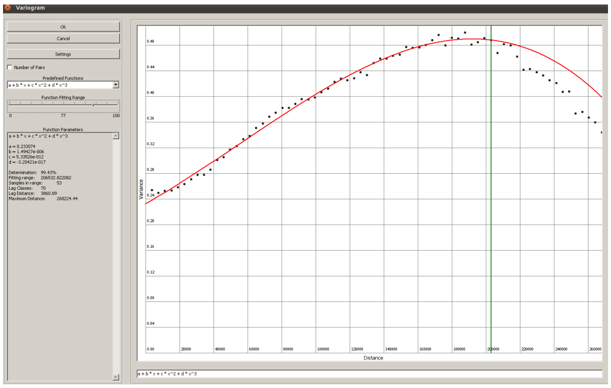

Figure 40: Variogram of the same dataset3 adjusted to the summit of the autocorrelation.

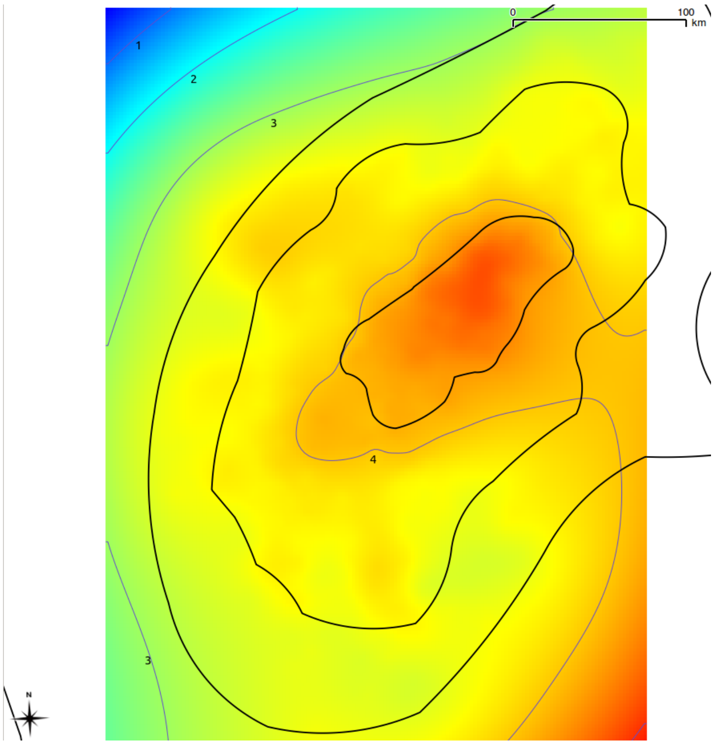

Figure 41: Isoseismal corresponding to the varigram adjusted to the summit of the autocorrelationof dataset3

The adjustment of the variogram on the range allows to move the isoseismals I, II and III closer to epicenter. The isoseismal IV remains adjusted on the isoseismal V of expert interpretation (bold line around the red zone). There is thus no improvement for isoseismal of value IV. Indeed, the adjustment of the variogram on the central values is bad. This induces a bad interpolation of the values around the epicenter.

8. References

8.1. Publications:

Bakun W. H., A. Gómez Capera, M. Stucchi (2011) Epistemic Uncertainty in the Location and Magnitude of Earthquakes in Italy from Macroseismic Data, Bulletin of the Seismological Society of America, v. 101 no. 6 p. 2712-2725.

Baumont D. et O. Scotti , (1999). Calibration en Ms et Mw d'une relation d'atténuation en intensité pour l'estimation des caractéristiques des séismes historiques en France métropolitaine, Bureau d'évaluation des risques sismiques pour la sûreté des installations, IRSN, 7ème colloque national AFPS, .

Bretherton, F.B., R.E. Davis and C.B. Fandry. (1976). A technique for objective analysis and design of oceanographic experiments applied to MODE-73. Deep-Sea Res., 23, 559-582.

Cara M, Schlupp A, Sira C (2007) Observations sismologiques : Sismicité de la France en 2003, 2004, 2005, Bureau Central Sismologique Français, ULP/EOST-CNRS/INSU, Strasbourg, 200p.

Cara M., W. Brüstle, M. Gisler, P. Kästli, C. Sira, C. Weihermüller et J. Lambert, (2005). Transfrontier macroseismic observations of the Ml=5.4 earthquake of February 22, 2003 at Rambervillers, France, Journal of Seismology, 9, p. 317-328.

Carr J. R. and Ch. E. Glass (1985) Treatment of earthquake ground motion using regionalized variables, Mathematical Geology, Volume 17, Number 3, 221-241.

Davis, J. C. (1986). Statistics and Data Analysis in Geology. 2nd ed, John Wiley & Sons. New York, 289 p.

De Rubeis, V., Gasperini, C., Maramai, A., Murru M., et Tertulliani A., (1992). The uncertainty and ambiguity of isoseismal, maps. Earthquake engeneering and Structural Dynamics, Vol 21, 509-523.

De Rubeis et al. (2005) Application of Kriging Technique to Seismic Intensity Data, Bulletin of the Seismological Society of America, Vol. 95, No. 2, pp. 540–548.

Deutsch, C.V. et A.G. Journel. (1992). GSLIB - Geostatistical Software Library. Oxford Univ. Press, New York, 340 p.

Dubrule, O. (1984). Comparing Splines and Kriging. Computers & Geosciences, 10(2-3): 327-33.

Gandin, L.S. (1965). Objective Analysis of Meteorological fields. Israël Program for Scientific Translations, No. 1373, 242 p.

Gasperini P. , G. Vannucci, D. Tripone, E. Boschi (2010) The Location and Sizing of Historical Earthquakes Using the Attenuation of Macroseismic Intensity with Distance, Bulletin of the Seismological Society of America, v. 100 no. 5A p. 2035-2066

Giovanni CARDENAS (Novembre 2004) .Utilisation du module « Geostatistical Analyst » d'ARCVIEW dans le cadre de la qualité de l'air . INERIS

Gratton, Y. et C. Lafleur . (2001). Le Matlab Kriging Toolbox. Version 4.0. Manuel de référence, INRS-ETE. Le logiciel est disponible gratuitement à l'adresse suivante : http://www.inrs-ete.uquebec.ca/activites/repertoire/yves_gratton/krig.htm

Gratton, Y., L. Prieur, R.G. Ingram, et C. Lafleur. (2002). Les courants en mer d'Alborán Est pendant la campagne Almofront-I. Rapport interne, INRS-ETE.

Journel, A.G. and C.J. Huijbregts. (1978). Mining Geostatistics. Academic Press, 600 p.

Krige, D.G. A statistical approach to some basic mine valuation problems on the Witwatersrand. (1951). J. of Chem., Metal. and Mining Soc. of South Africa, 52, 119-139.

Liebelt, P.B. (1967). An introduction to Optimal Estimation, Addison-Wesley, 267 p.

Marcotte, D. (1991). Cokriging with MATLAB. Computers & Geosciences, 17(9): 1265-1280.

Maruyama Y. and F. Yamazaki (2006) Relationship between seismic intensity and drivers' reaction in the 2003 Miyagiken-Oki earthquake Structural Eng./Earthquake Eng., JSCE, Vol. 23, No. 1, 69s-74

Matheron, G. (1972). Theorie des variables regionalisees, in Traite d'Informatique Geologique, Masson, Paris, 306–378.

Matheron, G. (1963). Principles of Geostatistics. Economic Geol., 58, 1246-1268.

Musson, R. M. W. (2000). Intensity-based seismic risk assessment, Soil, Dyn. Earthquake Eng. 20, 353–360.

Musson R. M. W. and M. J. Jiménez (2008) Macroseismic estimation of earthquake parameters, NERIES project report, Deliverable NA4-D3: Procedures for macroseismic estimation of earthquake parameters, http://emidius.mi.ingv.it/neries_NA4/docs/NA4_D3_v2_2.pdf.

Pasolini C., P. Gasperini D. Albarello, B. Lolli, V. D'Amico (2008) The Attenuation of Seismic Intensity in Italy, Part I: Theoretical and Empirical Backgrounds, Bulletin of the Seismological Society of America, v. 98 no. 2 p. 682-691

Schenková Z., V. Schenk, I. Kalogeras, R. Pichl, P. Kottnauer, C. Papatsimba and G. Panopoulou (2007) Isoseismal maps drawing by the kriging method, Journal of Seismology, Volume 11, Number 1 , 121-129.

Sirovich L., F. Cavallini, F. Pettenati and M. Bobbio (2002) Natural-Neighbor Isoseismals, Bulletin of the Seismological Society of America, v. 92 no. 5 p. 1933-1940

Thywissen K and J. Boatwright (1998) Using safety inspection data to estimate shaking intensity for the 1994 Northridge earthquake, Bulletin of the Seismological Society of America, v. 88 no. 5 p. 1243-1253.

Tselentis G-A. and E. Sokos, (2012) Relationship between isoseismal area and magnitude of historical earthquakes in Greece by a hybrid fuzzy neural network method, Nat. Hazards Earth Syst. Sci., 12, 37–45, doi:10.5194/nhess-12-37-201

8.2. Web sites:

http://www.sppsr.ucla.edu/up206b/Interpolation_methods.htm, A few Interpolation methods (Collected and organized from ArcMap Help files)

http://help.arcgis.com/en/arcgisdesktop/10.0/help/index.html#/Understanding_interpolation_analysis/009z0000006w000000, ArcGis Resource Center

Date: 8 May 2012

Review of the report:

« Methodological studies for isoseismal analysis »

By A. Schlupp, Ch. Sira and M. Durrenberger

Review by Thierry Camelbeeck

The purpose of this note is to review briefly the preliminary report by Schlupp, Sira and Durrenberger presenting the background information and the first methodological developments for the analysis of earthquake isoseismals in the framework of the Sigma project.

AIM OF THE STUDY

The final objectives of the study are to determine relationships between isoseismal areas and magnitude/depth parameters in France from well-constrained data and to furnish the methodological background to apply the method to well-documented recent earthquakes but also to older seismic events for which the data quality is less strong.

Using isoseismal areas to evaluate earthquake source parameters is different from the most recent developed methods like Boxer or the one of Bakun and Wentworth. It will be interesting at the end of the project to compare the different approaches, particularly for earthquakes with a poor intensity dataset.

The aim of the part of the study presented in the preliminary report concerns the adequate choice of methods to generate automatically isoseismals based on observed intensities.

RAMBERVILLERS DATA USED FOR THE METHODOLOGICAL DEVELOPMENT

On one hand, I thank the authors for the clarity in the presentation of the different used methods. On the other hand, the presentation of the datasets used for the different tests should be presented in more details.

The presentation of the dataset is incomplete because only the geographical location of the intensity data points (IDP) and the isoseismal expert drawings are presented. I recommend adding other information under the form of maps, graphics and (or) tables:

(1) The earthquake macroseismic map with the whole intensity dataset and the isoseismals drawn by the BCSF experts (perhaps a global map + one map at the same scale that the ones presenting the different automatic processing.

(2) A detailed statistical analysis of the dataset: (a) number of IDP per intensity classes; (b) repartition of the IDP with distance by intensity classes; (c) …

PRELIMINARY RESULTS

In the report, the quality of the automatic drawing is quantified in two ways:

- The visual comparison of the automatic drawing with the BCSF expert drawing;

- The comparison of areas of the isoseismals for each intensity level for the different datasets.

The visual comparison, even if it can help to evaluate quickly if the result is good or not, does not allow evidencing the relative quality of the different results obtained with the different methods on the different datasets.

The comparison of the areas of the isoseismals is difficult to analyze without any comparison to what is expected in the more favorable cases.

Therefore, I recommend:

(1) To better explain how to interpret the comparison with isoseismal areas [perhaps by furnishing the values of areas corresponding to the average, median and 0.84 percentile of the distance distribution for each intensity value?];

(2) To define a real estimator of the discrepancy between IDP and the automatic isoseismal drawings.

I agree completely with the preliminary conclusions of the work:

(1) The Voronoï diagram is not adapted for the purpose of the work;

(2) More work is necessary to characterize the differences in the results with the IDW and Kriging. This needs a good estimator of the drawing quality.

Two comments on the figures:

- The correspondence between color and intensity should appear on the different maps;

- Figures 29 and 38 are not legible

Di
S
G
G

UNIVERSITÀ DEGLI STUDI DELLA BASILICATA
DIPARTIMENTO DI STRUTTURE, GEOTECNICA,
GEOLOGIA APPLICATA ALL'INGEGNERIA
Viale dell'Ateneo Lucano, 10 - 85100 Potenza - Italy
Tel. +39 0971 205102/4/5/6 - Fax +39 0971 205070

Review of the document: **SIGMA-2012-D3-36**
Toward the definition of reference ground-motion by Laurendau *et al*.

Performed by: **Marco Mucciarelli, Università della Basilicata**

The reviewed report describes the present advancement of studies aimed to define standard rock motion at a reference site and to implement a methodology to calculate reference ground-motions via a stochastic approach.

The data and the methodologies used are in advance to the state of the art (e.g., the Stockwell transform instead of the Short Time Fourier Transform). The work is still in progress and the authors correctly identify possible improvements.

There are some open questions, reported in the following.

1) In the introduction the authors refer to the work of Cadet et al (2010), recognising that Vs30 could be a poor proxy of seismic amplification and that predominant period is at least equally important. This idea was proposed/supported using different data set also by Gallipoli and Mucciarelli (2008), Castellaro et al. (2008) and Di Alessandro et al (2012). In this last paper one of the authors is also among the authors of the reviewed report. Why here they have decided to ignore Fo and consider only Vs30?

2) The choice of Vs30>500 m/s as characteristic of a "rock" condition seems questionable. In

literature is possible to find paper describing resonant/amplifying behaviour of sites with much larger Vs30, see as example the NEHRP-classB (760<Vs30<1500 m7s) sites in Taiwan (Sokolov et al., 2007). I understand the need for a larger data set, but in this way is possible to obtain an unwanted effect: to include in GMPEs the effect of intermediate to low frequency amplification, that may result in the observed mismatch with stochastic simulation.

3) The data set used is composed of recordings with different sampling ratio and thus with different Nyquist frequency. How were they filtered to avoid bias in 1st order moment estimation? Moreover, if NyF=50 Hz (0.02 s), why some graph include empirical estimates in the range 0<T<0.2 s (e.g., fig. 20)?

4) When choosing the coefficients for the negative exponential trend of the central frequency the author states that "*we take the values of the A and B coefficients from the S-wave part, or then the P-wave part if B is positive*". In this case ***k*** has to do with P-waves and it is possible that being related to attenuation it could be influenced by the fact that Qp=9/4Qs, thus being little representative of S-waves attenuation.

5) It is not clear why in Tab 3 the GMPE for different parameters were derived for different combination of ground motion (independent, geometric or arithmetic mean).

The supposed relationship between ***k*** and Vs30 has a correlation coefficient of just 0.018, and the graph shows clearly that varying Vs30 there is no variation for ***k***. How it possible to say that there is a significant relationship between the two variables?

6) I probably missed something or plainly misunderstood the sentence "*Figure 27 (top) shows the 30 time histories that have the best match with the target spectrum over the whole period range, and Figure 27 (bottom) over the period range from 0.01 s to 0.3 s. Note that using this method, the selected time histories show a better fit at long periods*." If the TH were selected to have the best match over the whole period range it seems obvious that they have a better match at lower periods than those selected for the best match at high periods only.

7) In the discussion, it is not clear if the overestimation of displacements at long period is attributed

to non-zero mean displacements and velocity or to some other reason. If it is the case, a standard de-trending and pass band filtering after each iteration can solve the numerical problem without requiring a filter linked to some physical property like the corner frequency.

References

Cadet, H., Bard, P., and Rodriguez-Marek, A. (2010). Defining a standard rock site: Propositions based on the KiK-net database. Bulletin of the Seismological Society of America, 100(1):172– 195.

Castellaro S., F. Mulargia and P. L. Rossi (2008) Vs30: Proxy for Seismic Amplification?; Seismological Research Letters; 8 v. 79 no. 4 p. 540-543

Di Alessandro C., L. F. Bonilla, D. M. Boore, A. Rovelli, O. Scotti (2012) Predominant‐Period Site Classification for Response Spectra Prediction Equations in Italy, Bulletin of the Seismological Society of America, vol. 102 no. 2 680-695.

Gallipoli M. R., Mucciarelli M. (2009) Comparison of site classification from VS30, VS10, and HVSR in Italy. Bull Seismol Soc Am., 99:340–351.

Sokolov V. Y., C.-H. Lohb, W-Y. Jean (2007) Application of horizontal-to-vertical (H/V) Fourier spectral ratio for analysis of site effect on rock (NEHRP-class B) sites in Taiwan; Soil Dynamics and Earthquake Engineering Volume 27, Issue 4, Pages 314–323.